SANDIA REPORT

SAND2013-10411
Unlimited Release
Printed November 2013

Ultra-Thin, Temperature Stable, Low Power Frequency References

Kenneth E. Wojciechowski, Roy H. Olsson III, Michael S. Baker

Prepared by
Sandia National Laboratories
Albuquerque, New Mexico 87185 and Livermore, California 94550

Sandia National Laboratories is a multi-program laboratory managed and operated by Sandia Corporation, a wholly owned subsidiary of Lockheed Martin Corporation, for the U.S. Department of Energy's National Nuclear Security Administration under contract DE-AC04-94AL85000.

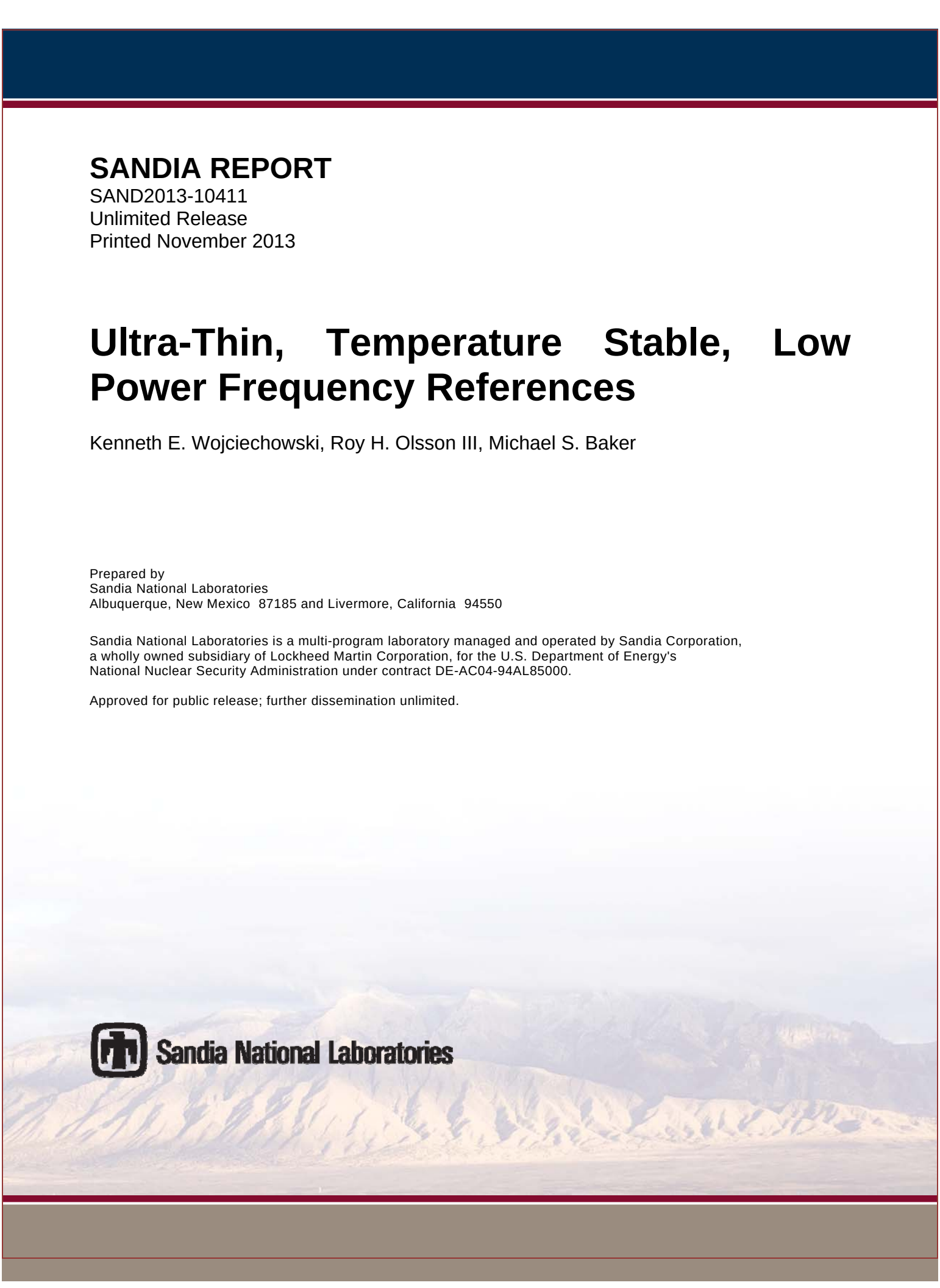

Issued by Sandia National Laboratories, operated for the United States Department of Energy by Sandia Corporation.

Available to DOE and DOE contractors from
U.S. Department of Energy
Office of Scientific and Technical Information
P.O. Box 62
Oak Ridge, TN 37831

Telephone: (865) 576-8401
Facsimile: (865) 576-5728
E-Mail: reports@adonis.osti.gov
Online ordering: http://www.osti.gov/bridge

Available to the public from
U.S. Department of Commerce
National Technical Information Service
5285 Port Royal Rd.
Springfield, VA 22161

Telephone: (800) 553-6847
Facsimile: (703) 605-6900
E-Mail: orders@ntis.fedworld.gov
Online order: http://www.ntis.gov/help/ordermethods.asp?loc=7-4-0#online

SAND2013-10411
Unlimited Release
Printed November 2013

Ultra-Thin, Temperature Stable, Low Power Frequency References

Kenneth E. Wojciechowski
Advanced Microelectronics and Radiation Effects
Sandia National Laboratories
P.O. Box 5800
Albuquerque, New Mexico 87185-MS1072

Roy H. Olsson III, Michael S. Baker
MEMS Technologies,
Sandia National Laboratories
P.O. Box 5800
Albuquerque, New Mexico 87185-MS1069

Abstract

We have developed a MEMS based thin (<100 μm), temperature stable (< 1 parts-per-billion per degree Celsius(ppb/°C)), low power (<10 mW), frequency reference. Traditional high stability oscillators are based on quartz crystals. While a mature technology, the large size of quartz crystals presents important mission barriers including reducing oscillator thickness below 400 μm, and low power temperature stabilization (ovenizing). The small volume microresonators are 2 μm thick compared to 100's of microns for quartz, and provide acoustic/thermal isolation when suspended above the substrate by narrow beams. This isolation enables a new paradigm for ovenizing oscillators at revolutionary low power levels <10 mW as compared to >300 mW for oven controlled quartz oscillators (OCXO). The oven controlled MEMS oscillator (OCMO) takes advantage of high thermal isolation and CMOS integration to ovenize the entire oscillator (AlN resonator and CMOS) on a suspended platform. This enables orders of magnitude reductions in size and power as compared with today's OCXO technology.

ACKNOWLEDGMENTS

The authors would like that thank the MDL staff at Sandia National Laboratories, especially Peggy Clews, and Tammy Plyum for their work fabricating the oscillators. This project was supported by Laboratory Directed Research and Development, Sandia National Laboratories, U.S. Department of Energy, under contract DE-AC04-94AL85000. Sandia National Laboratories is a multi-program laboratory managed and operated by Sandia Corporation, a wholly owned subsidiary of Lockheed Martin Corporation, for the U.S. Department of Energy's National Nuclear Security Administration under contract DE-AC04-94AL85000.

CONTENTS

FIGURES

TABLES

NOMENCLATURE

°C	Degrees Celsius
°K	Degrees Kelvin
3D	Three Dimensional
ADEV	Allan Deviation
Al	Aluminum
ALC	Automatic Level Control
AlN	Aluminum Nitride
ANSYS	Engineering Simulation Software, www.ansys.com.
CAD	Computer Aided Design
CMOS	Complementary Metal Oxide Semiconductor
CMOS7	Sandia National Laboratories internal radiation hardened CMOS process
COTS	Commercial Off-The-Shelf
CRTCL	Constant Resistance Temperature Control Loop
dB	Decibel
dBc	Decibels normalized to oscillator carrier power.
DOE	Department of Energy
E	Youngs Modulus
G	Acceleration where G = 9.8 m/s^2
GHz	10^9 Hertz or gigahertz
GPa	Pressure in 10^9 pascals or gigapascals
IC	Integrated Circuit
k	Thermal conductivity in watts per meter per kelvin
kg	kilograms
kHz	10^3 Hertz or kilohertz
mA	10^{-3} amps or milliamps
MEMS	Micro Electro-Mechanical Systems
MHz	10^6 Hertz or megahertz
mm	Distance in millimeters
μm	Distance in micrometers
MESA	Microsystems and Engineering Sciences Applications
mTorr	10^{-3} Torr or milliTorr
mW	10^{-3} Watts or milliwatts
MEMS Pro	Engineering design software, www.softmems.com/mems_pro.html
NDK	NIHON DEMPA KOGYO Company, LTD.
NW	Nuclear Weapons
OCMO	Oven Controlled MEMS Oscillator
OCXO	Oven Controlled Crystal Oscillator
OPAMP	Operational Amplifier
PCB	Printed Circuit Board
pF	10^{-12} Farads or Picofarads
ppb	Parts per billion
ppm	Parts per million
PR	Photo Resist
PTAT	Proportional to absolute temperature

Q	Resonator Quality Factor
ρ	Density in kg/cm^3
RIE	Reactive Ion Etch
SiO_2	Silicon Di-Oxide
SNL	Sandia National Laboratories
SOI	Silicon On Insulator
TCE	Temperature Coefficient of Expansion
TCF	Temperature Coefficient of Frequency
TCR	Temperature Coefficient of Resistance
TCXO	Temperature Compensated Crystal Oscillator
V	Voltage
W	Power in Watts
WLP	Wafer Level Packaging
Ω	Resistance in Ohms
XeF_2	Xenon Di-Fluoride

\

1. INTRODUCTION

Over the past 3 years Sandia National Laboratories has been developing a replacement for Ovenized Crystal Oscillator (OCXO) frequency references. OCXOs are high quality frequency references second only to their cousins the atomic clock in terms of stability. They provide high spectral purity and high accuracy output frequencies, exhibit exceptional long term aging, (parts per million per year) and have low sensitivity to ambient temperature drift (parts per billion, per degree Celsius, ppb/°C). Crystal oscillator manufactures go to great lengths to provide ppb/°C temperature drift performance. To obtain such high levels of stability, ovenized crystal oscillators have oven(s)integrated directly within their package. Inside the package of a ovenized crystal oscillator both the electronics and crystal resonator are commonly positioned inside the oven chamber along with a temperature sensor and a heater (Figure 1).

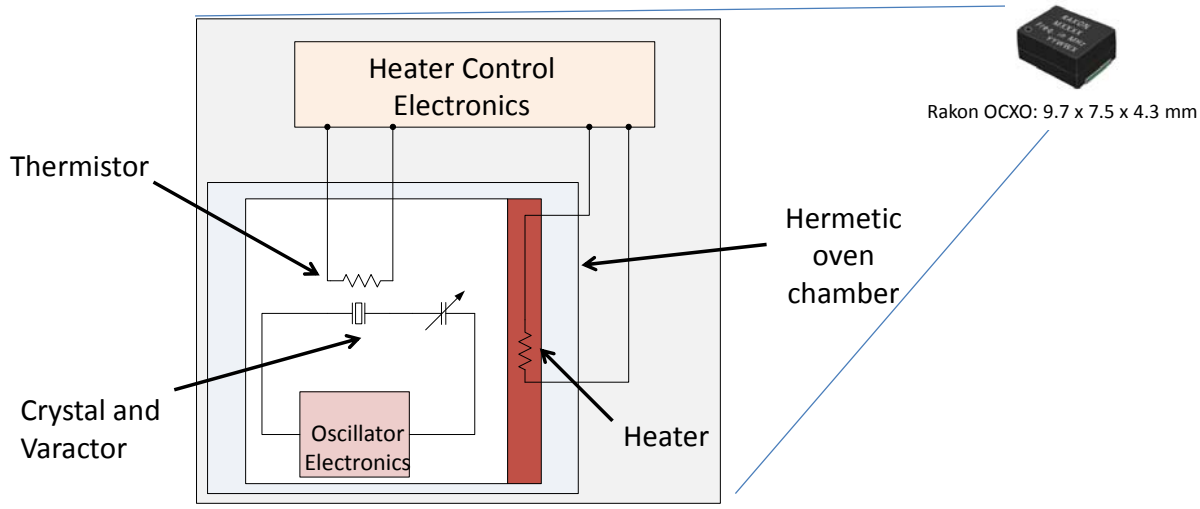

Figure 1. Example of existing technology: Oven controlled Quartz Oscillators, OCXOs

The chamber is then thermally regulated at a temperature greater than the crystal oscillator assembly's maximum specified operating temperature. The ability to minimize changes in chamber temperature due to changes in ambient temperature is measured by a metric referred to as oven gain. Oven gain is the ratio of the change in ambient temperature divided by the corresponding change in the oven chamber's temperature. Sometimes two chambers are used to obtain better isolation or oven gain by placing one oven inside of another. One can imagine that it requires large power consumption to heat these chambers. That is where thermal isolation becomes important. Thermal isolation or thermal resistance is a measure of how much power is required to heat the oven above ambient. Typical OCXOs cannot achieve very high thermal resistances due to size constraints of the package, electronics and quartz crystal. Hence, they can easily use watts of power to heat up to their internal operating temperature and require 100's of milli-watts, mW, to maintain it. This leads to another metrics for OCXO's: warm up time. Due to their size and hence volume, OCXOs have large heat capacities. Thus, OCXOs have long thermal time constants (1-10 minutes) and can take 10's of minutes to warm up [1,2]. This makes

them slow to react and they cannot compensate for quick changes in ambient temperature. While a mature technology, the large size and mounting of quartz crystals presents important mission barriers including: reducing oscillator thickness below 400 µm, ovenizing for maximum temperature stability at low power, and shock induced frequency shifts arising from the large crystal mass.

At the micro scale (sub one milli-meter dimensions) one can readily obtain high thermal resistances. Thermal resistances of 50 degrees Celsius per mW, °C/mW, and higher are easily obtained. In addition the small volume of these devices results in low heat capacities. The resulting thermal time constants, (1 to 100 milli-seconds) can be 1000's of times smaller than what is obtained with today's OCXOs. Hence, the power required to heat these devices can be considerably less and the temperature of the device can be controlled at a much greater rates. This is the basis of our LDRD project and our big technology advantage. To implement an OCXO at the micro scale we are leveraging the ability to integrate aluminum nitride, AlN, resonators directly with our 0.35 µm CMOS process, CMOS7 [3,4]. This is a capability that is unique to our Sandia National Laboratories MESA fabrication facility. It is a post CMOS process and the AlN resonators are deposited on top of a completed CMOS wafer. This provides the ability to make very small oscillators. (500 µm long, 500 µm wide and 14 µm thick). Figure 2a is an example of the integration technology. It consists of a 532 MHz ring resonator fabricated directly on top of a pierce oscillator in Sandia National Laboratories CMOS process.

a)

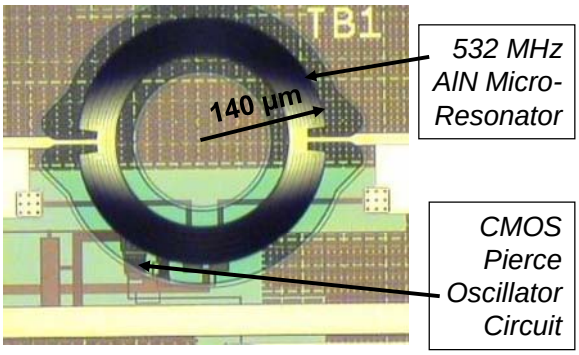

b)

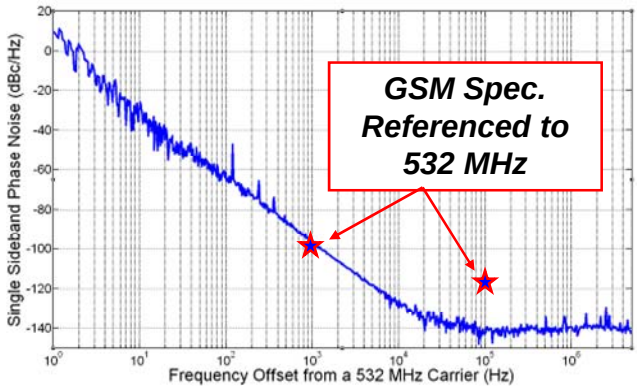

Figure 2. a) Picture and b) Phase Noise of a 532 MHz AlN Oscillator Integrated Directly Over CMOS [3]The goal of this LDRD (Table 1) was to develop a frequency reference with cross-

cutting applicability across Sandia's missions. For many missions size, power and temperature stability are of upmost importance. Thus the goal was to develop a thin (< 100 μm), low power (< 10 mW), temperature stable (<10 parts-per-billion (ppb), frequency reference over -40°C to 85°C. The investigation included modeling and experimentation of ovenized resonators with different anchoring suspensions, heaters, and sensors to minimize oven and circuit power while maintaining resonator performance and maximizing temperature stability. This LDRD has demonstrated a multi-frequency low noise ovenized oscillator technology with unprecedented frequency stability over temperature (< 1 ppb) at low power (5-10 mW). The size of these novel devices is less than 2 mm^2 and they can be thinned to less than 100 μm thick. Therefore, the resulting volume of the device can be as low as 0.2 mm^3.

Table 1: State of the Art Frequency References and LDRD Goals

Vendor Product	Technology	Frequency (MHz)	Phase Noise 1kHz offset (dBc/Hz) ref. 1 GHz	Vibration Sensitivity (ppb/G)	Power (mW)	Temp. Coeff. (ppb/°C)	Volume(mm^3)
Rakon RFPO40	Ovenized Quartz (OCXO)	10.94	**-105**	**2**	**400**	±0.5 to ±2 (ramp rate: 1°C/min)	**313**
NDK NT3225SA	Temp. Comp Quartz (TCXO)	10-26	N/A	N/A	4.5	48	7
Si Labs Si530	TCXO + PLL	622.08	-103	N/A	280	112	58
Si Time SiT8003XT	Electrostatic MEMS	50	-44	N/A	10	800	2.6
Previous Sandia AlN on CMOS	Piezo MEMS	20,80, 100, 530	-90	N/A	6	2000	0.06
LDRD Goals	Ovenized Piezo MEMS	10-1500	**-90**	**0.01**	**<10**	**0.14**	**0.06-1**

2. TECHNICAL APPROACH

2.1. Temperature Dependence of an Oscillator

To understand oscillator temperature dependence it is important to note that an oscillator is a positive feedback loop (Figure 3a) comprised of a frequency determining element (resonator) and a gain element (oscillator electronics). An oscillator's dependence on temperature is a complex function of many variables. However, there are three main variables that usually dominate and they are physical properties of the resonator. The first is the temperature dependence of the resonator center frequency on temperature. This temperature dependence can be linear or nonlinear. For AlN resonators it can be approximated by Eq. 1. This describes how the center frequency of the resonator, f_{res}, changes with temperature. The most important term in this Eq. is typically the first order or linear temperature coefficient of frequency, TCF_{res}. However in a resonator that has been temperature compensated the resonator's frequency may have a 2nd order or higher order nonlinear variation with temperature. The coefficents are typically normalized. For instance, the linear term, TCF_{res}, has units of parts per million per degree Celsius or ppm/°C and the 2nd order term has units of ppm/(°C)^2. Note that T_{res} is the temperature of the resonator and f_o is the center frequency of the resonator at T_{res} = 0 °C.

$$f_{res}(T_{res}) = f_o \times \left(1 + TCF_{res} \times T_{res} + TCF2_{rss} \times {T_{res}}^2\right) \tag{1}$$

The second important characteristic of the resonator is its quality factor or Q. The resonators quality factor is a measure of the steepness or slope of the phase difference between its input and output current when sweeping its drive voltage input frequency through the resonators' resonance (figure 3b). The steepness of this slope directly affects how sensitive the oscillator's frequency output is to phase changes which occur in the oscillator electronics. For the oscillator shown in Figure 3, one can derive the condition for oscillation. This occurs when two conditions are met at the same time. First, the negative real impedance of the oscillator electronics is equal to the motional impedance of the resonator, R_x. This is equivalent to the requirement of unity loop gain for stable output amplitude in classical oscillator theory. Second, the total phase in the oscillator loop is zero or a multiple of 360 degrees. These two conditions are met [5] when the real and imaginary impedances of the resonator, Z_{res}, and the oscillator electronics, Z_{elect} sum to zero (Eq. 4). Note that IM_{elect} is the imaginary impedance of the oscillator electronics and is typically sensitive to temperature.

$$Z_{res} = R_x + j\omega L_x + \frac{1}{j\omega C_x} \tag{2}$$

$$Z_{elect} = -R_x + j\ IM_{elect}(T_{elect}) \tag{3}$$

$$Z_{res} + Z_{elect} = 0 = j\omega L_x + \frac{1}{j\omega C_x} + jIM_{elect}(T_{elect}) \tag{4}$$

Solving Eq. 4 for the frequency, f_{osc} (note $\omega = 2\pi f_{osc}$), at which oscillation occurs as a function of the imaginary impedance of the oscillator, IM_{elect}, results in the first term of Eq. 5. It is assumed $f_{osc} = f_o$ in this case. This term defines the oscillator's sensitivity to temperature due to changes in the oscillator electronics' temperature, T_{elect}. The second term defines the oscillator sensitivity

due to changes in the resonators temperature, T_{res}. Typically these two temperatures are not the same but both vary with the ambient temperature of the entire oscillator, $T_{ambient}$. From Eq. 5 it is clear that the sensitivity of an oscillator to temperature is inversely proportional to the resonator's phase slope at resonance (slope = – 2Q) and to its motional impedance. Interestingly, this analysis yields the third physical property which affects temperature stability; the motional impedance of a resonator. It implies that as the motional impedance is increased relative to the imaginary impedance, IM_{elect}, the less sensitive the oscillator is to changes in IM_{elect}. Variation in the electronics due to temperature can cause oscillator sensitivities in the range of 1 ppb/°C for oscillators with resonator quality factors in the millions [6]. For oscillators using AlN resonators which have quality factors in the range of 1000 to 2000, the oscillator electronics can result in variation on the order of 1 ppm/°C. However, if temperature compensation of the electronics is performed to reduce variation in IM_{elect} it is feasible to reduce this variation significantly. It is also worth noting that if the resonator is not temperature compensated, its TCF can easily dominate the oscillator's variation over temperature. For example, uncompensated AlN resonators have linear temperature coefficients in the range of –20 to –30 ppm/°C.

$$\frac{\Delta f_{osc}(Temperature)}{f_{osc}} \cong -\frac{IM_{elect}(T_{elect})}{2Q\,R_x} + TCF_{res} \times T_{res} + TCF_{2res} \times T_{res}^{\ 2} \tag{5}$$

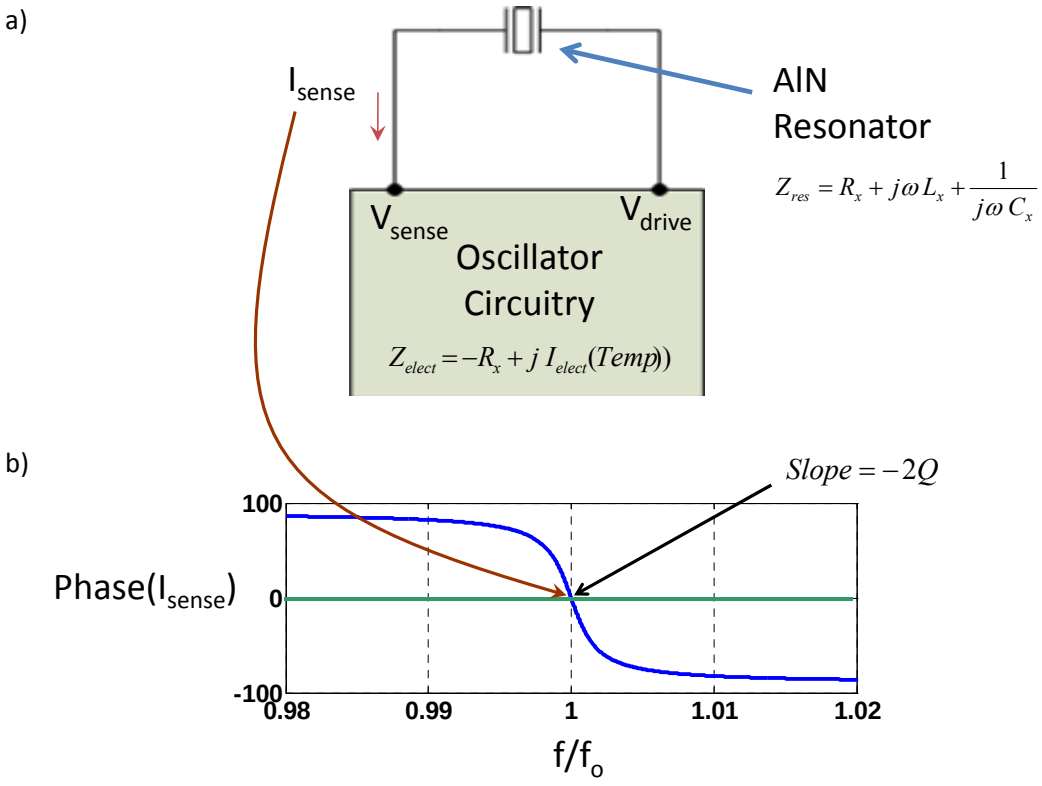

Figure 3: a) Functional diagram of an oscillator and representation of the resonator and circuitry as impedances. b) Phase between input drive voltage, V_{drive}, and I_{sense} versus normalized frequency. Assumes V_{sense} is at a virtual ground.

2.2. PCB Based oscillators with Thermally Stabilized or "Ovenized" Resonators and Resonator Platforms

Our initial approach to achieve improved oscillator thermal stability was to thermally stabilize or "ovenize" the resonator only (Figure 4a) while using temperature compensated oscillator electronics. This was based on the fact that the resonator is the dominate source of temperature instability in the oscillator. Therefore, thermal stabilization of the resonator was expected to improve the overall oscillator stability. The PCB is shown in Figure 4b. The approach incorporated an AlN resonator on an "oven" platform designed to allow control of its temperature at a fixed set point that was selected to be above the maximum ambient temperature that the device would be expected to operate at.

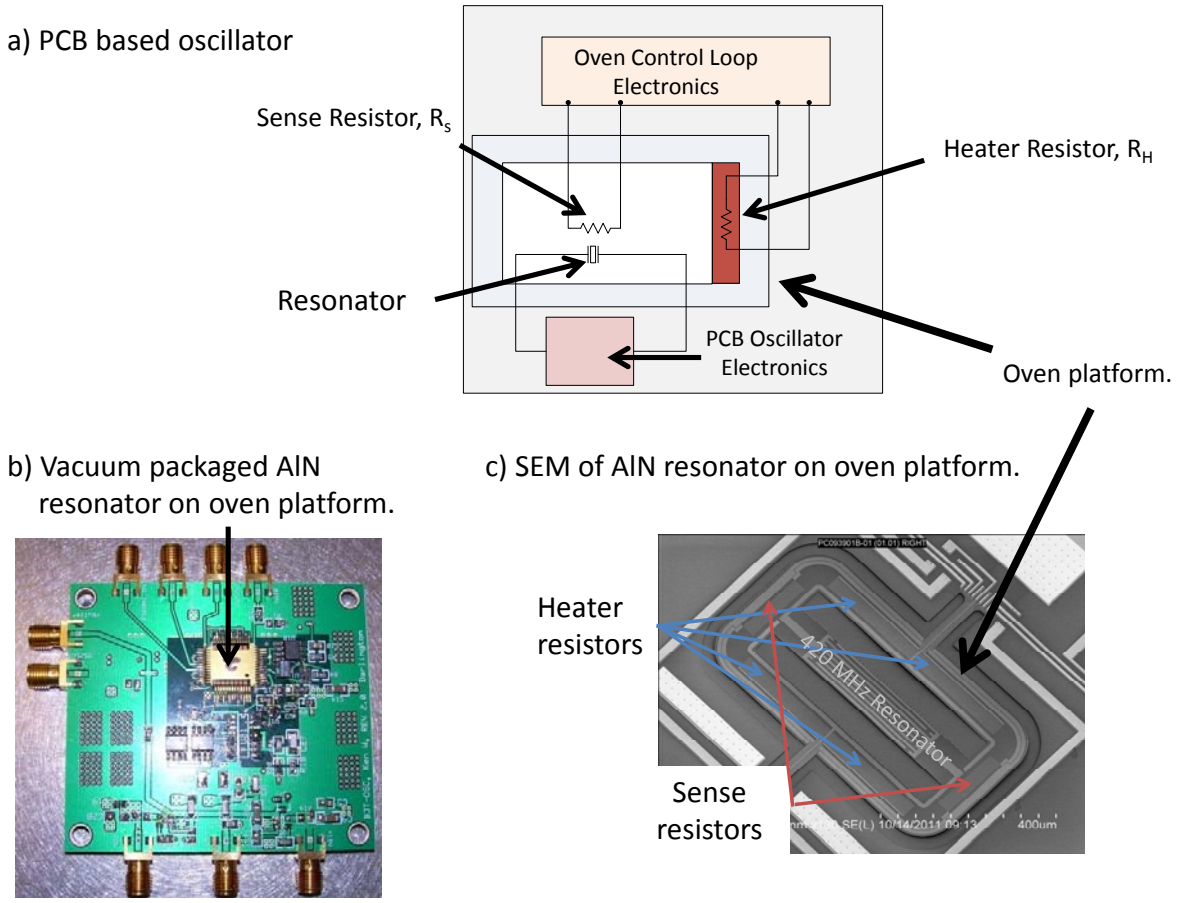

Figure 4: First demonstration of a resonator with built in heaters [7].

2.2.2. Thermally Stabilized or "Ovenized" Resonators and Resonator Platforms

Thermal stabilization using the platform similar to Figure 4c and Figure 5 made a few basic assumptions. First, by placing the platform in high vacuum the only path for heat loss is through the platform and its support beams. Therefore, it assumes heat loss due to both convection and radiation is negligible. Second, the temperature at the points where the resonator is connected to the platform is held at a constant temperature. Third, the temperature at these points is assumed to be equal due to the symmetry of the platform. It is assumed that holding the value of sense resistance, $R_s = R_{s1} + R_{s2}$, constant forces the temperature of the sense resistors R_{s1} and R_{s2} to a

constant value. Moreover, through placement of the heater resistors in the positions shown in figures 4c and 5 we can ensure there is no temperature gradient across the sense resistor. Hence, the points at which the resonator is connected to the platform can be held at a temperature independent of the ambient conditions (Figure 5). This is the basis of a constant resistance temperature control loop (CRTCL). The CRTCL measures the temperature of the device by measuring an aluminum sense resistor or thermistor, R_s, (Figure 4b, 5) on the platform. The loop controls the average temperature of the sense resistors, $T_{platform}$, by applying power to the heater resistors, $R_{H1\text{-}4}$. It adjusts the temperature of the sense resistors such that their value is equal to an off-chip reference resistor, R_{ref}, which typically has a 0.2 ppm per degree Celsius temperature coefficient of resistance, TCR. The connections between the resonator and the oscillator electronics are made through RESIN and RESOUT.

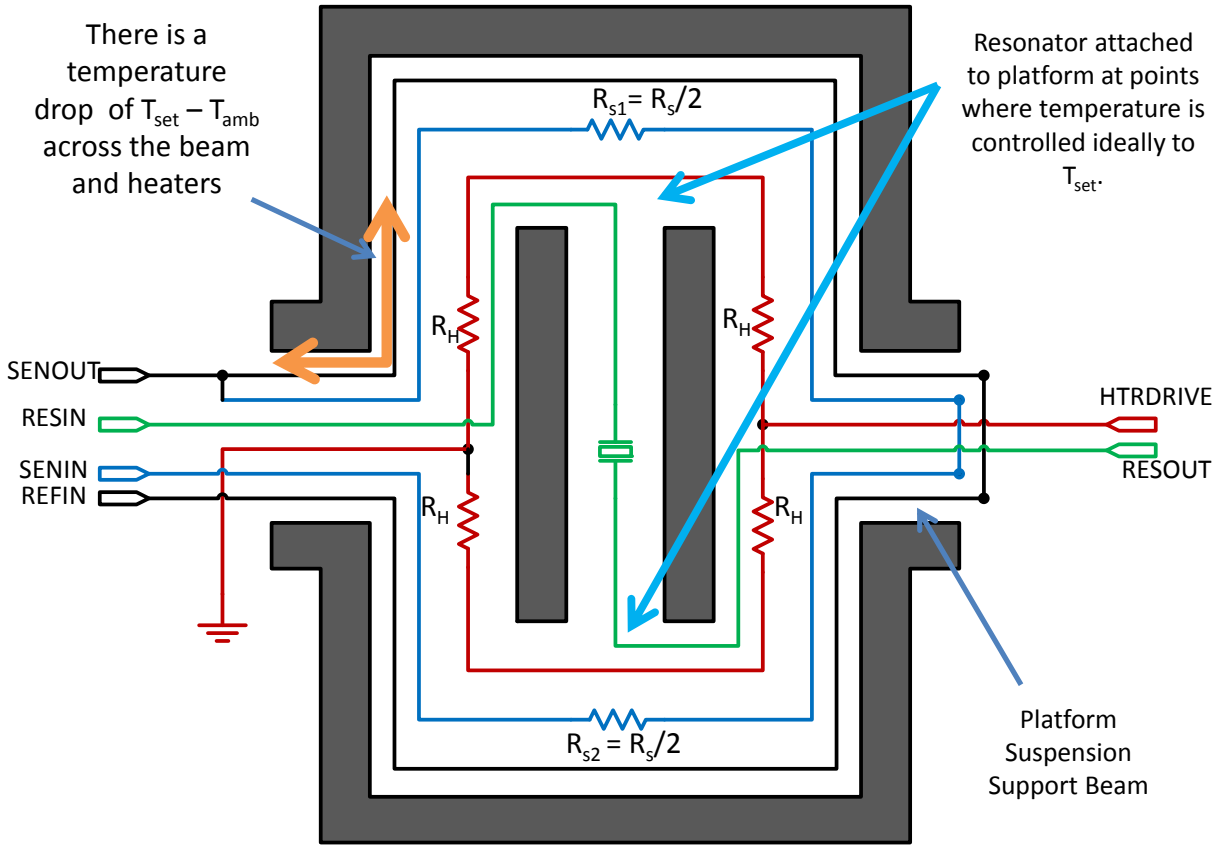

Figure 5: Schematic drawing of the platform used to thermally isolate the AlN resonator. Heater (R_H) and sense resistors (R_{s1} and R_{s2}) are located such that heat loss due to conduction can be eliminated. RESIN and RESOUT are the input and output of the resonator on the platform.

Measurement and control of the sense resistances value is critical for good control of the platform and hence resonator temperature. This measurement is complicated by the existence of the metal traces that route to them. These traces have a significant parasitic resistance, R_{spar}, when compared to the sense resistance. In addition, they route over areas where there are temperature gradients that are dependent on the ambient temperature. The total sense resistance from SENIN to SENOUT (Figure 5) is given by Eq. 6.

$$R_{sTot} = R_{s1} + R_{s2} + R_{spar} = R_s + R_{spar} \tag{6}$$

To enable the measurement of R_s independent of this parasitic trace resistance, R_{spar}, an additional metal trace or reference path was added to the platform. The reference path is shown by the connection between REFIN to SENOUT in figure 5. The reference path resistance $R_{refplat}$ was designed such that its resistance could be measured in order to cancel out the effect of R_{spar} on the total sense resistance. Therefore, the reference path resistance on the platform, $R_{refplat}$, has a value given by Eq. 7.

$$R_{refplat} = R_{refpar} + R_{refl} = R_{spar} + R_{refl} \tag{7}$$

$$R_{refTot} = R_{refplat} + R_{ref} \tag{8}$$

Note the platform reference resistance has two components. The first component has a value, R_{refpar} which is ideally matched to R_{spar}. The second is the part of the metal trace, R_{refl}, that routes over or adjacent to R_{s1} and R_{s2}. It is assumed that this resistance is at the same temperature as the sense resistors and therefore does not contribute to an ambient temperature dependent error. The total reference resistance is the sum of the off-chip reference resistor, R_{ref}, and $R_{refplat}$ (Eq. 8).

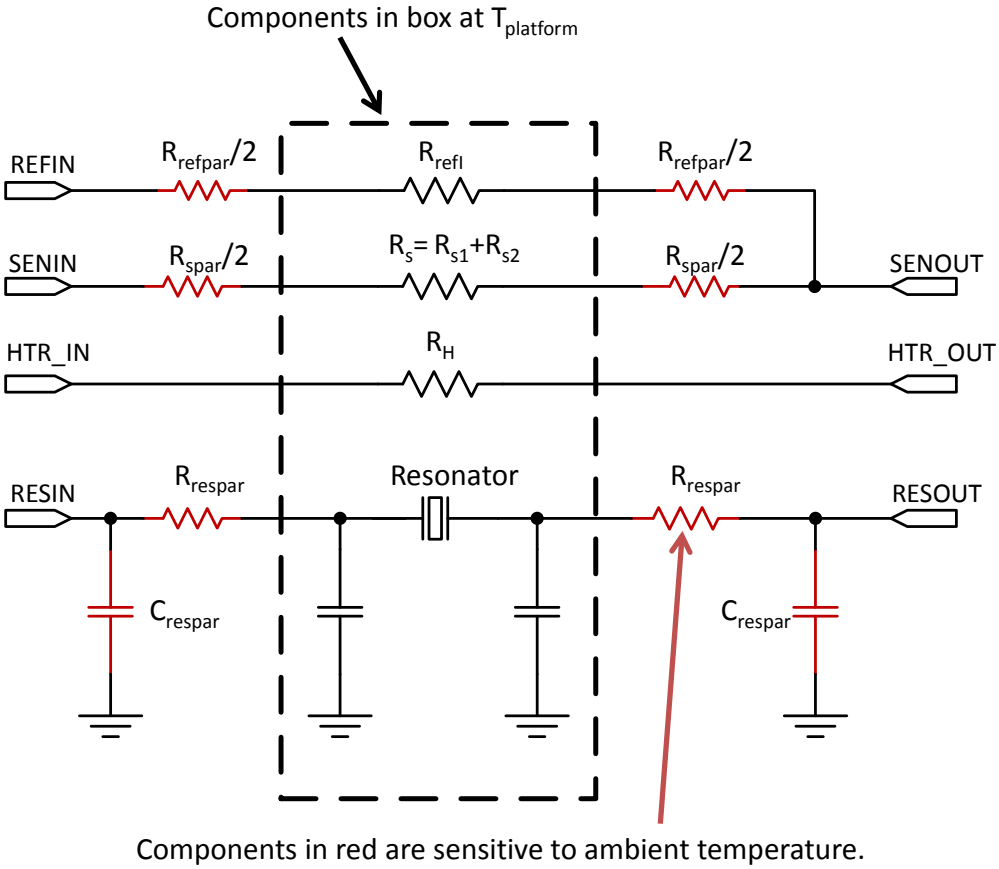

Figure 6. Ovenized platform electrical model. It includes parasitics for both the oven control loop and the resonator.

A schematic diagram of the CRTCL is shown in Figure 7. The loop operates by setting the sense resistance, R_{sTot} equal to R_{refTot}. This is done by first calculating V_{sense} (Eq. 9) with OPAMP1. Then, the integrator formed by OPAMP2 and the components R_1, R_2 (Note $R_1 = R_2$) and C_1 forces $V_{sense} + V_{ref} = 0$, (Eq. 10). In Eq. 11, Eq. 10 is simplified to find the value of the sense resistance forced by the loop. Note that if the parasitic resistances $R_{spar} = R_{refpar}$ the sense resistance will not be a function of temperature. The resulting temperature of the resonator or $T_{platform}$ (Eq. 14) can by calculated using Eq.s 11, 12 and 13 and assuming $R_{refpar} = R_{spar}$, $R_{refI} << R_{ref}$ and the control loop has infinite gain at DC. Where T_{set} is the desired temperature set point and G_{oven} is the oven gain. Oven gain is a measure of how well the oven rejects changes in ambient temperature.

$$V_{sense} = -\frac{R_{refTot}}{R_{sToT}} V_{ref} \tag{9}$$

$$V_{ref} + V_{sense} = V_{ref} + \left(-\frac{R_{refTot}}{R_{sToT}} V_{ref} \right) = 0 \quad \Rightarrow \quad R_{sToT} = R_{refTot} \tag{10}$$

The control loop forces the condition : $R_s = R_{ref} + R_{refI} + R_{refpar} - R_{spar}$ (11)

$$R_s = R_{s0C}\left(1 + TCR_S T_{platform}\right) \tag{12}$$

$$R_{ref} = R_{ref\,0C}\left(1 + TCR_{ref} T_{amb}\right) \tag{13}$$

$$T_{platform} = T_{set} + \frac{1}{G_{oven}} T_{amb} = \frac{R_{ref\,0C} - R_{S0C}}{R_{s0C} TCR_S} + \frac{R_{ref\,0C}}{R_{s0C}} \frac{TCR_{ref}}{TCR_S} T_{amb} \tag{14}$$

R_{s0C} and R_{ref0C} are the values of the sense resistor and reference resistors at zero degrees Celsius. The typical TCR or TCR_S for the aluminum sense resistor is ~4000 ppm per degree Celsius. As noted previously the TCR for the off-chip reference resistor, TCR_{ref}, is ~0.2 ppm per degree Celsius. For typical values the oven gain can be as high as 12,000. This means a 1 degree change in ambient temperature results in $1/12{,}000^{th}$ of a degree Celsius change in platform temperature. The effective temperature coefficient of frequency, $TCF_{effective}$, for a resonator placed on the thermally stabilized platform is given by Eq. 15.

$$TCF_{effective} = \frac{TCF_{res}}{G_{oven}} = \frac{-20\,\frac{ppm}{°C}}{12000} \cong -1.7\,\frac{ppb}{°C} \tag{15}$$

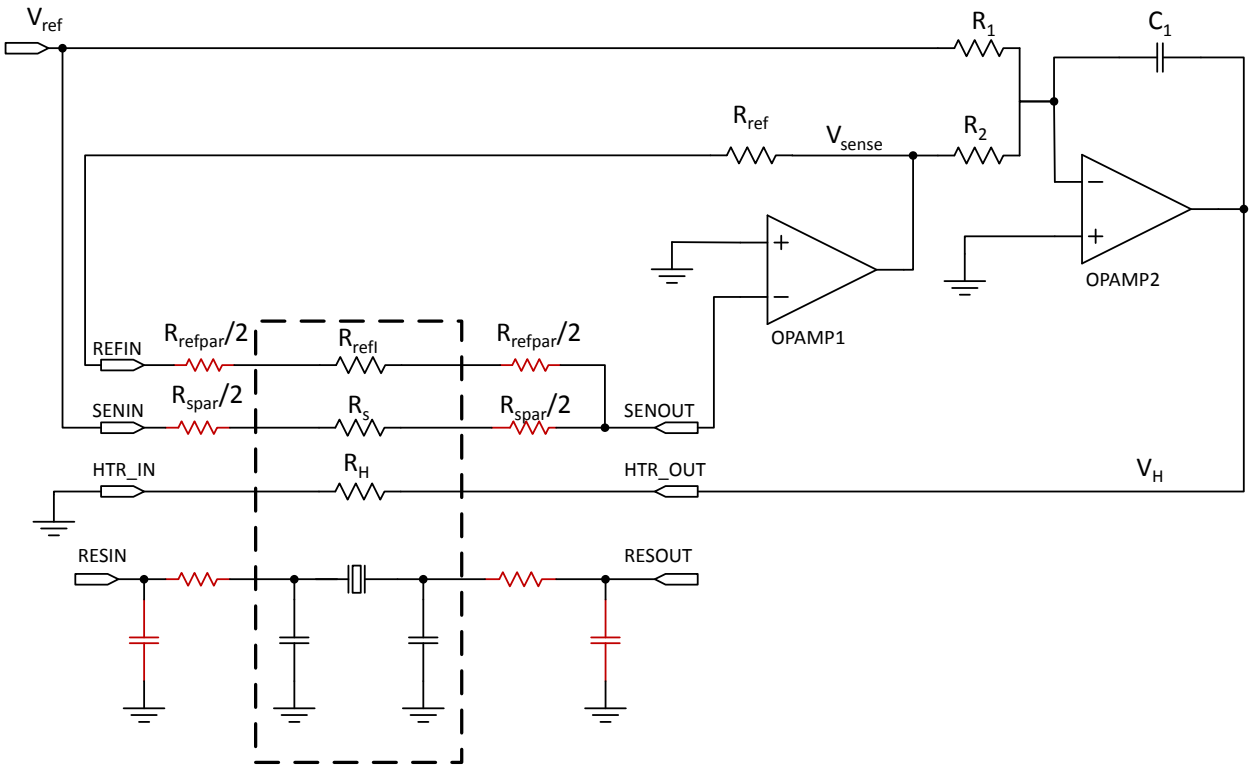

Figure 7: Constant resistance control loop. This loop forces $R_{sTot} = R_{refTot}$.

2.2.3. PCB based Ovenized MEMS Oscillator Results

A 45 MHz COTS based oscillator and heater control loop were developed with a platform similar to Figure 4c. The temperature in the room was varying by ~ 1 degree Celsius with a two hour period. This can be seen in the frequency versus time measurement of the oscillator in Figure 8. This oscillator achieved a *TCF* of -1.7 ppm/°C. The resonator is in a vacuum package shown in Figure 8. The effective TCF of the device was expected to be much better than -1.7 ppm/°C given the resonators *TCF* was –20 ppm/°C and an oven gain of twelve thousand. In addition, the same resonator was measured open loop, i.e. not in the oscillator. The measurement yielded a *TCF* of -0.64 ppm/°C with the thermal control loop on. Based on these results it was concluded that several factors were causing the large *TCF* after thermal stabilization.

Factors leading to poor thermal stability:

1. The oscillator electronics were introducing temperature sensitive frequency variation which was not rejected by the resonator due to its relatively low quality factor, Q, which is in the range of ~ 1000 to 2000 for AlN devices.
2. Parasitic resistance, R_{respar}, and capacitance, C_{respar}, due to the trace routing from the resonator to the oscillator circuitry is a function of ambient temperature and contributes to the large *TCF* (see Figure 6).

3. Heat loss due to poor vacuum levels (> 1 Torr) in the package and/or radiative heat loss was limiting the oven gain of the control loop. This is especially important if the resonator has a large *TCF*.

Hence, oscillator stability over temperature was believed to be limited by multiple factors. To address these factors, especially items 1 and 2 above, we developed the world's first Oven Controlled MEMS Oscillator or OCMO. The OCMO will be discussed in detail in the following sections.

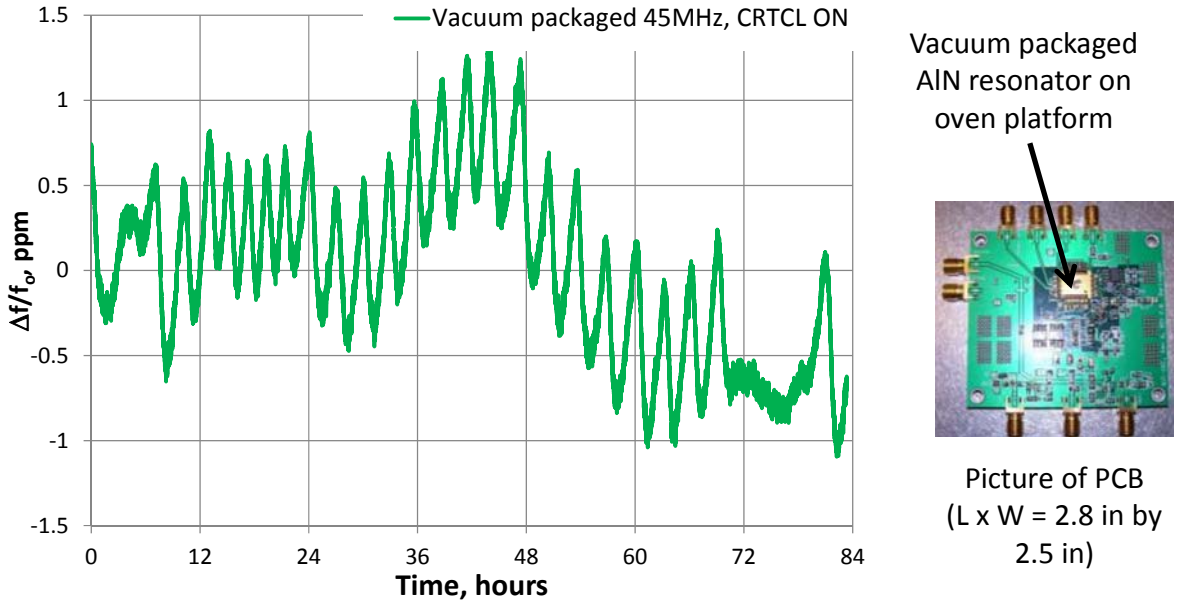

Figure 8. Frequency Measurement of PCB based in a COTS vacuum package PCB Oscillator Loop.

2.3. Ovenized MEMS Oscillator (OCMO): Concept and Fabrication Process

The discoveries in the PCB based design led to the concept and development of a fully ovenized MEMS oscillator or OCMO on a single integrated circuit, IC, chip. A drawing of the OCMO platform and photograph of the OCMO IC fabricated at Sandia National Laboratories is shown in Figure 9. To implement this OCMO at the micro scale we are leveraging the ability to integrate aluminum nitride, AlN, resonators directly with our 0.35 μm CMOS process, CMOS7. This is a capability that is unique to our Sandia National Laboratories MESA fabrication facility. It is a post CMOS process and the AlN resonators are deposited on top of a completed CMOS wafer. This provides the ability to make very small thermally isolated oscillators. The actual OCMO platform in the IC is 730 μm long, 500 μm wide and 14 μm thick. The support beams connecting the platform to the IC are ~500 μm long. The fabrication process is a low temperature post CMOS process where AlN resonators are deposited directly on top of a completed CMOS wafer. Following deposition of the AlN resonators, a platform is defined by etching down through the AlN and CMOS stack to the silicon handle wafer. This platform is then released from the silicon substrate. A heater resistor and metal temperature sense resistor are integrated into the platform. They provide the ability to control the platform temperature.

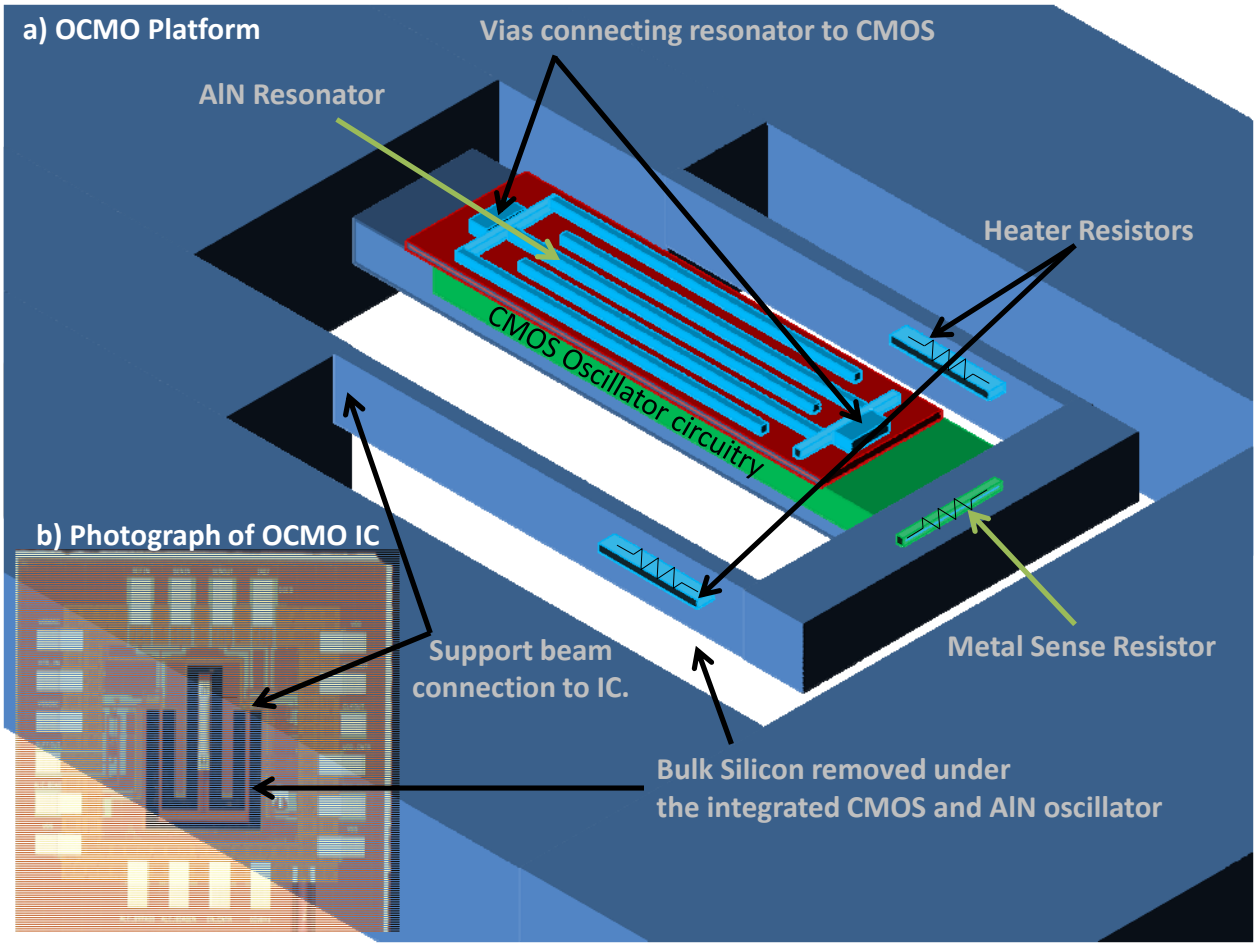

Figure 9. a) Drawing of OCMO oven platform. b) Photograph of OCMO IC. IC size L x W x H = 1.8 mm x 1.8 mm x .7 mm.

The only connection to the substrate is through support beams (Figure 9). In vacuum (sub 10 milli-Torr) the thermal resistance of the structure can be controlled by the dimensions of the support beam. Note that this structure maintains the temperature of the oscillator constant similarly to the platform show in Figure 5 through the placement of the heater resistors and sense resistor to ensure heat loss due to conduction is eliminated. Typically, it is set at a temperature slightly above the maximum desired operating temperature of the device. In vacuum we have achieved thermal resistances that result in a 26 degrees Celsius increase in platform temperature using only 1mW of power. Hence only a few milli-watts are needed to stabilize the platform at 125 degrees Celsius over −55 to 85 °C. By placing our device in a chip scale vacuum package the entire OCMO will have a volume of less than 1 mm^3.

The basic building blocks of the OCMO are:

- Thermal stabilization or "ovenization" of the oscillator electronics as well as the AlN resonator by placing them on a thermally isolated platform.
- An AlN resonator that is temperature compensated. Most importantly the temperature compensation must be done such that turnover point of the resonator *TCF* [8] is at the planned temperature set point, T_{set}, of the platform.

By ovenizing the oscillator electronics, thermal variation due to the oscillator electronics (factor 1) is eliminated. By placing the resonator directly above the oscillator circuitry the thermal variation due to trace routing is eliminated. Therefore its advantages over the PCB based design are:

- We do not need "high resonator Q" and can live with Q ~ 1000 and still achieve high temperature stability. This is because the oscillator circuitry is thermally stabilized (e.g. "ovenized").
- The interconnect between the oscillator electronics and resonator is thermally stabilized.

While the OCMO thermal platform design removes temperature instabilities due to the electronics and trace routing it does not solve temperature variation due to poor vacuum or radiative heat loss. Poor vacuum and/or radiative loss provides a path for heat to flow between the outside world and the resonator. Hence, even if the control loop keeps the sense resistors at a constant temperature, the resonator temperature can still vary. In other words, while the oven gain at the sense resistor may be 12,000, it can be much less at the resonator. This problem can be solved in three ways, all of which can all be implemented at the same time.

1. Develop an AlN resonator with a very low TCF.
    a. Place the turnover point of the TCF at the planned temperature set point of the platform. This greatly relaxes the required oven gain.
2. Co-locate the sense resistor and resonator. Theoretically this should improve the oven gain because the control loop will be directly observing and controlling the resonators' temperature. However, co-location places restrictions on the value/size of resistance that can be obtained which can affect control loop performance.
3. Reduce vacuum levels in the package until heat gain/loss due to convection becomes negligible. This assumes radiative heat loss is not also a significant cause of instability.

In this work we have investigated all three methods. The best results were obtained by developing a low TCF resonator and using a sense resistor that is not co-located with the resonator. However, co-location of the sense resistor and resonator remains a very good option. Vibration stability is also another challenge met by the OCMO design. Typically, for oscillators with high levels of stability under vibration, sensitivity to vibration is limited by the electrical connections between the oscillator electronics and the resonator. Typically these connections, for example wire bonds, have electrical properties (inductance, capacitance, resistance) that are sensitive to vibration [9]. In the OCMO there is a direct connection between the oscillator electronics and the resonator. The mechanical resonance of this connection is in the 100's of kilohertz. Hence, it is much less sensitive to vibration. Furthermore, the resonator platform itself has a resonant frequency of 19 kHz. This makes it insensitive to most vibrations which exist at low frequency. In summary, the OCMO developed in this work addresses all factors leading to the thermal and vibration instability in order to obtain an oscillator that has performance comparable to today's state of the art OCXO with orders of magnitude improvement in size and power.

2.3.1. Fabrication Process to Create an Ovenized MEMS Oscillator (OCMO)

The OCMO fabrication process is a post-CMOS process where the AlN resonators are fabricated on top of CMOS wafers after they have completed CMOS fabrication. This process takes advantage of the CMOS7 trench isolated silicon-on-insulator, SOI, process. This CMOS7 process starts with an SOI wafer (Figure 10). Silicon islands are defined (Figure 10-2) where transistors or other silicon based devices will be formed (Figure 10-3). After the devices are formed, metal interconnect is patterned on top of the devices and an SiO_2 layer is deposited on top of the wafer (Figure 10-4). This completes the CMOS processing. By controlling the placement of the metal interconnects and Si devices we can create regions of CMOS circuitry that are completely encapsulated within silicon dioxide. This is the key to creating the isolated platforms as it enables the platform to be physically defined by etching through the SiO_2 to the bulk Si (Figure 10-5) and then performing a highly selective isotropic silicon etch (Figure 10-6). The bulk silicon substrate is removed during this etch while anything protected by SiO_2 is not. Hence, the transistors and other devices are preserved (Figure 10-6).

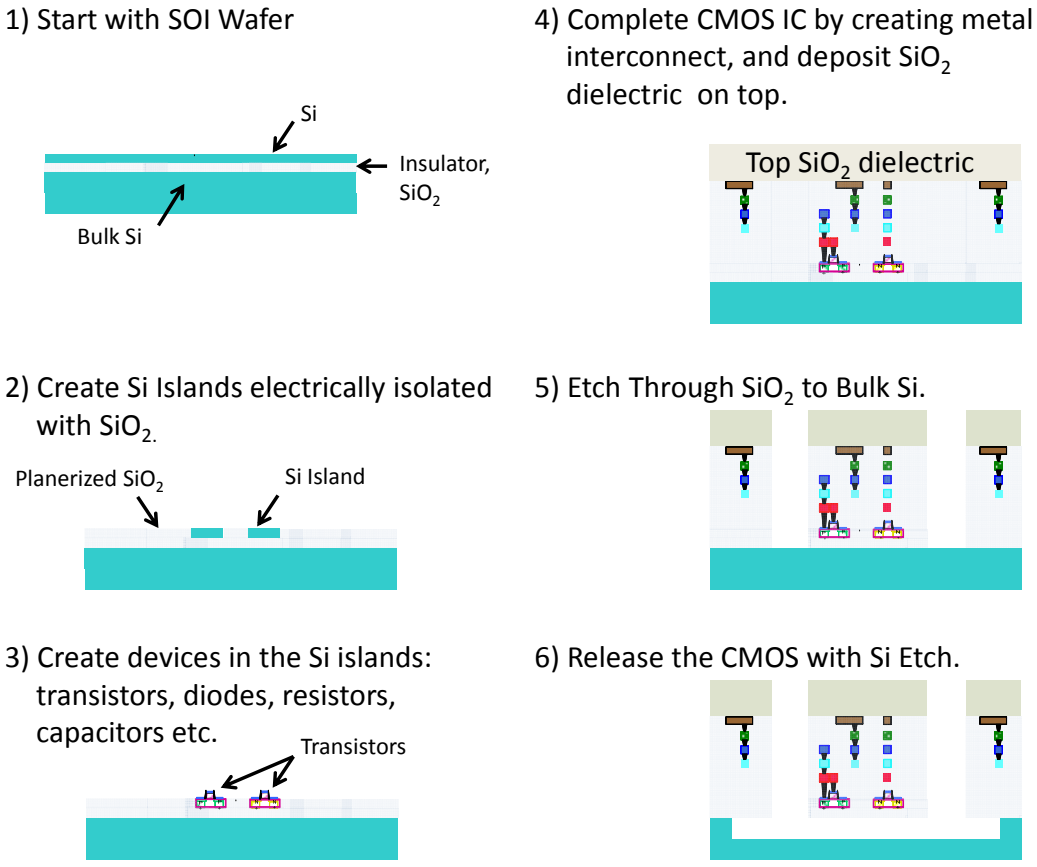

Figure 10: Process steps to create mechanically and thermally isolated structures in trench isolated SOI CMOS.

This is an example of the process steps required to create both thermally and mechanically isolated structures composed of trench isolated SOI CMOS electronics. To create an oscillator with AlN resonators additional process steps must be added. This requires adding the post

CMOS compatible aluminum nitride process to this flow (Figure 10) before steps 5 and 6 are completed. The additional process steps needed to add the AlN resonator and create the OCMO platform are shown in Figure 11. These process steps are described below:

Steps 1-2 (occurs after step 4 in Figure 10): The AlN resonators are defined using the process described in [4]. Note the resonator is not released. Also, there is an additional sub-step added to step 1 in this process where the oxide thickness under the resonator is adjusted to create a temperature compensated resonator. The turnover temperature of the oscillators' TCF is determined by this thickness.

Step 3: A single mask is then used to define the area where oxide will be etched down to the bulk silicon handle wafer. Photo resist is patterned, PR, and then an etch step removes the amorphous silicon in these area. The PR mask is left on for final etch in step 4.

Step 4 (replaces step 5 and 6 in Figure 10): Once the amorphous silicon is removed a reactive ion etch, RIE, is used to remove the oxide. The etch stops on the bulk silicon handle wafer. This defines the size and shape of the oven platform. After the RIE oxide-etch the PR is striped. The final step is the release of the AlN resonator and the entire platform using a XeF_2 etch to remove the amorphous silicon under the AlN resonator and the bulk silicon under the platform. Figure 11-4 shows the cross section of the OCMO after the release step. Note the bottom of the CMOS electronics are protected during release by the SOI buried oxide layer. The top and sides of the electronics are protected by the interlayer dielectric oxide used in the CMOS metal interconnect.

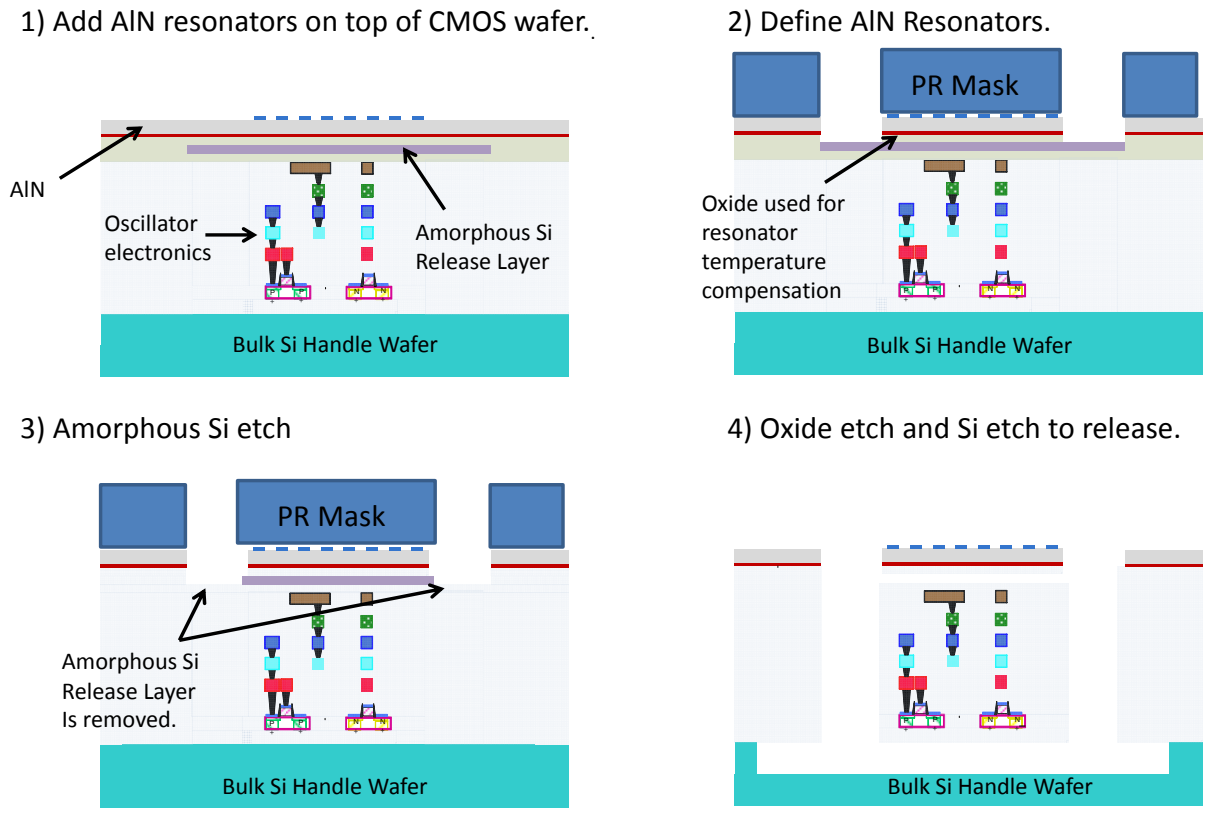

Figure 11. Additional Process steps needed to add AlN to the CMOS platform.

2.4. OCMO DESIGN

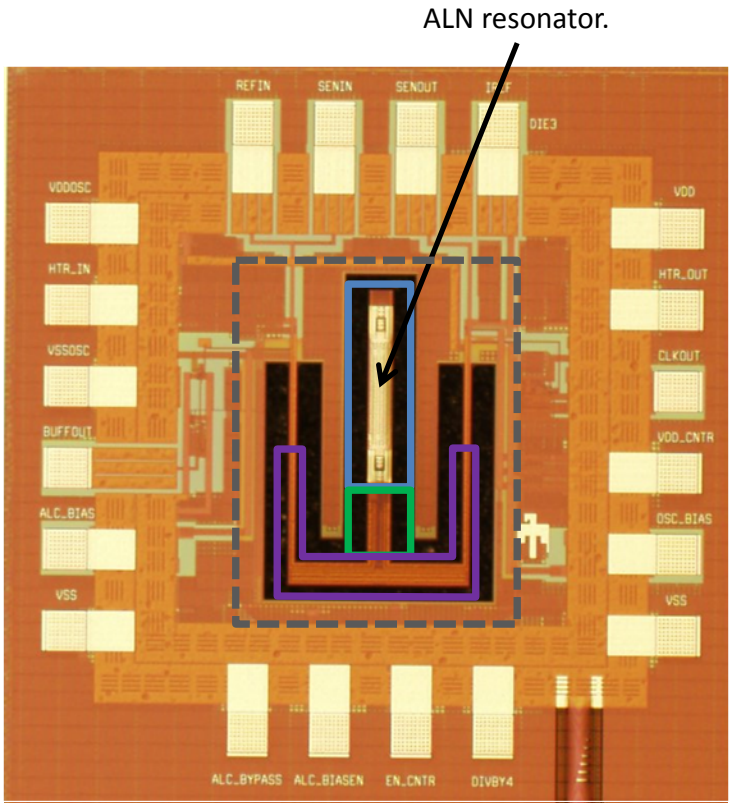

Figure 12. Picture of released OCMO indicating location of CMOS circuitry. The platform is approximately 730 μm long, 500 μm wide and 14 μm thick.

The grey dashed box indicates the thermally isolated OCMO platform. The purple box indicates the position of the resistive heater and sensor.

- The platform is designed to control the temperature of the oscillator electronics and AlN resonator.
- Poly silicon heater resistors are implemented in the CMOS platform. This removes the issue of electromigration from the heater.
- Metal sense resistors are used for platform temperature sensing.

The blue box indicates the CMOS circuitry directly under the AlN resonator. Including:

- A Pierce oscillator.
- An automatic level control, ALC, loop used to control the amplitude of oscillation.
- A proportional to absolute temperature, PTAT, current bias circuit used as an alternate method for platform temperature sensing

The green box contains the following circuitry:

- A dynamic counter with the option to divide by 32 or 40.
- Configuration logic to control the state of all the circuitry.

2.4.1. OCMO Platform Design

The OCMO platform design was built on the work done on the ovenized resonator platforms developed for the PCB based oscillators. To reduce complexity in this initial OCMO design, it

was decided to locate the thermal control loop electronics off-chip. The drawback to placing the loop on the PCB is power consumption and size. The advantage is that the loop can be changed without reprocessing the CMOS IC, thereby enabling flexibility in the initial development of the OCMO control loop. In future designs this loop could be implemented directly on the OCMO IC. A thermal schematic diagram of the OCMO platform is shown in Figure 13. The heater resistors are located such that there will be no thermal gradient across the sense resistor in the absence of convection or radiative heat loss. In addition, as described earlier, there is a reference path (REFIN to SENOUT) and sense path (SENIN to SENOUT) built into the platform to provide a means of cancelling out the parasitic resistance in the metal sense resistor path. The location of the PTAT current source is shown as well. The PTAT current source was designed as a backup temperature sensor. Its advantage is that the output current can be measured off chip and is not sensitive to trace routing. It is also not sensitive to electromigration for which the metal sense resistor can experience if not operated at a low enough current density. However, it is sensitive to power supply variation with temperature. In addition, it is noisier than the metal temperature sensor. Hence, it was not used for temperature control in the final oscillator. In addition, it was assumed that the average power used by the oscillator electronics on the platform is constant over temperature or has a small effect on the temperature of the oscillator with respect to the sense resistor temperature. Ostensibly, the oscillator power creates a fixed temperature gradient between the oscillator and sense resistor. The CMOS metal layers were used in the area where the resonator and oscillator are located to reduce the thermal resistance in order to make it as isothermal as possible and to minimize the temperature gradient between the oscillator and sense resistor. In future designs colocation of the resistive sensor with the oscillator will reduce effects of oscillator power variation.

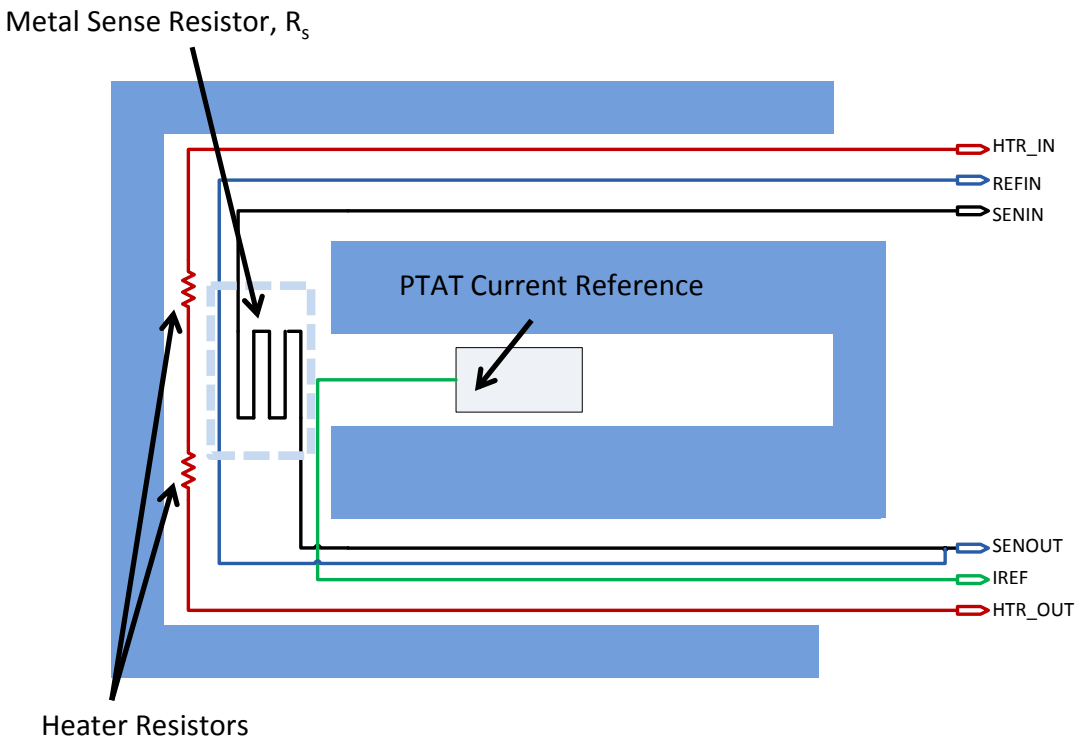

Figure 13. Schematic diagram of OCMO indicating electrical connections and locations of the sense resistor, heater resistors, and PTAT current reference.

A thermal model was developed in a computer aided design (CAD) package named ANSYS. The purpose of the model was to demonstrate the concept of creating an isothermal area on the OCMO platform. A process modeling tool available in MEMS Pro was used to generate a 3D model of the OCMO which was then exported to ANSYS. The platform design used to generate the model was simplified in order to enable convergence of the thermal model in ANSYS. The first thermal simulation using this model did not include the modeling of any radiation or convection related heat transfer (Figure 14). In addition, power consumption in the oscillator electronics were not modeled for simplification. Future models could include the power consumed by the oscillator electronics. The power applied to the heater resistor (2.86 mW) resulted in a temperature rise of 34 °C above the ambient temperature (22 °C). The effective thermal resistance of the device was calculated to be 11.9 °C/mW. Note that the resonator and oscillator electronics are in an isothermal region.

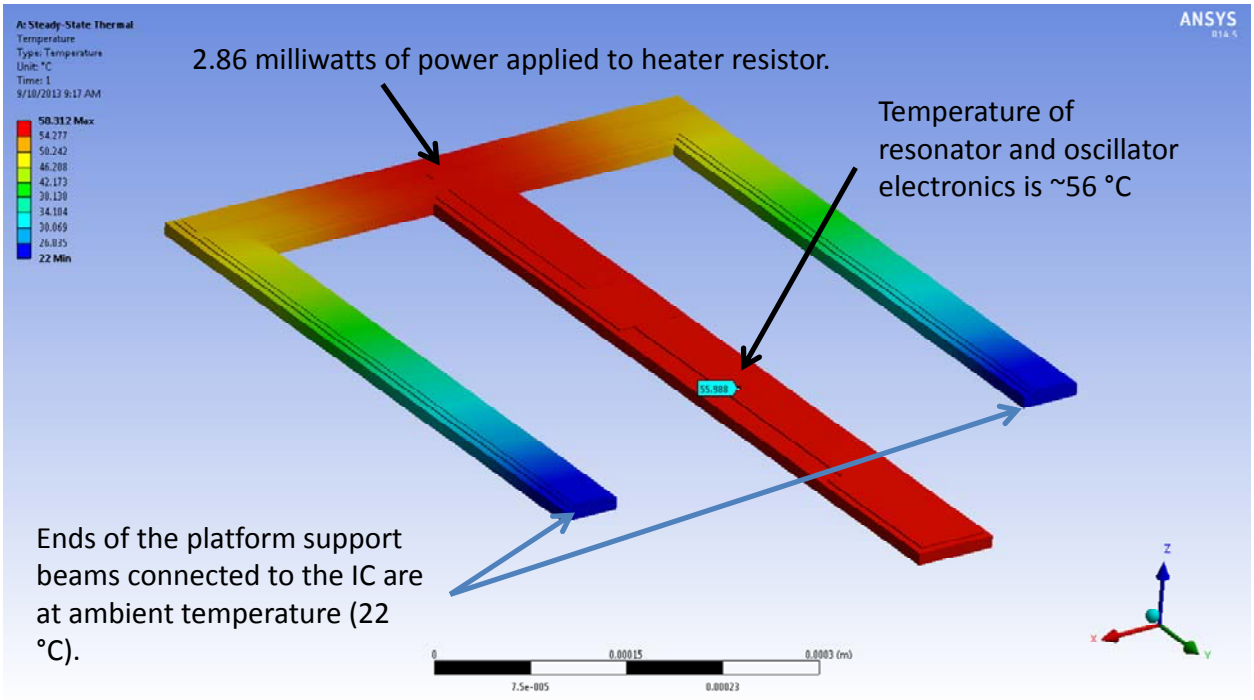

Figure 14. OCMO platform thermal model results with heat loss due to conduction only. The area where the oscillator and resonator are located is isothermal.

Table 2: Material parameters used in the ANSYS thermal analysis [7,13]

Layer	1	2	3
Material	Al	AlN	SiO_2
E,Young's Modulus (GPa)	69	342	75
ρ, density (kg/m^3)	3230	2700	2200
TCE, (ppm/°K)	–590	–37	185
k, thermal conductivity (W/m°K)	237	60	1.4

The second simulation performed adds radiative heat transfer to the model. The model used a surface emissivity of one which is worse case. The ambient temperature was set at 22 °C and the same power was applied to the heater in this simulation. As expected, a thermal gradient developed along the length of resonator and oscillator device. In addition, one can see a thermal gradient from the top to the bottom of the platform in the area where the oscillator is located. This implies radiation does limit the maximum oven gain that can be achieved and thus cannot be ignored.

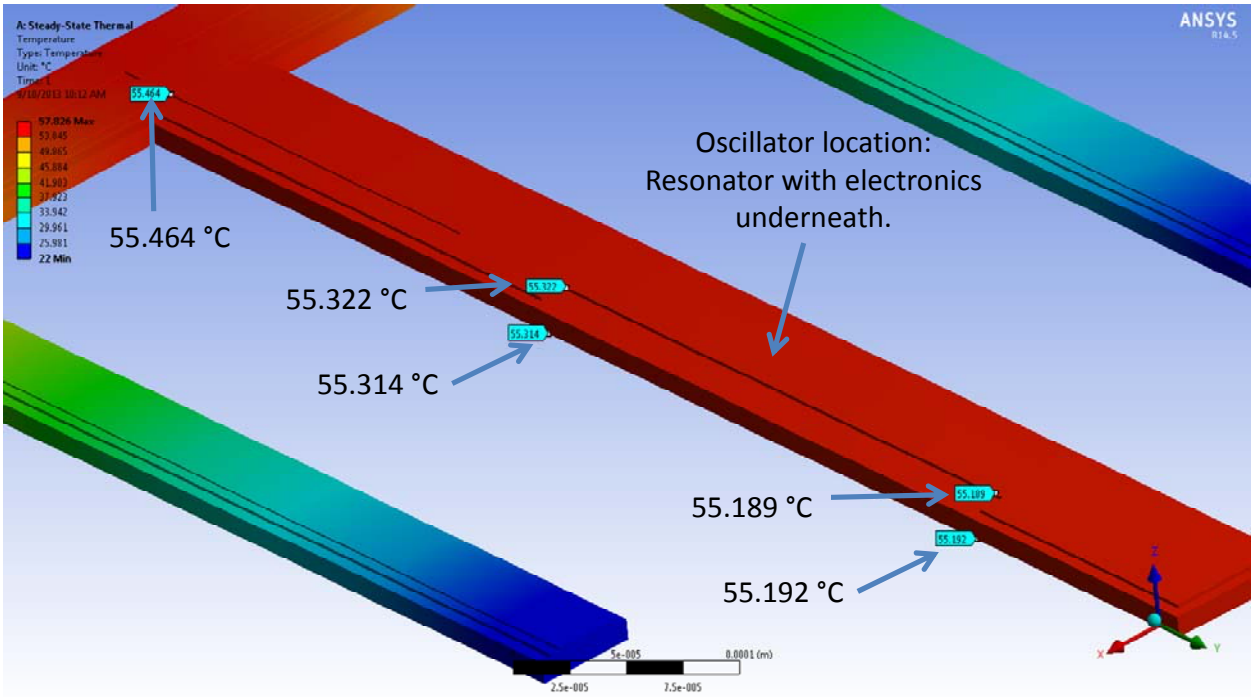

Figure 15. OCMO platform thermal model results with heat loss due to conduction and radiation.

To determine how much the oven gain is limited by radiation and convection, the heater resistor was set to a constant temperature and the platform's average emissivity, the vacuum package pressure, and the outside ambient temperature were varied independently. Therefore, the effects of these variables on the oven gain could be quantified for this platform. To look at the effect of convection, a 30 micrometer thick layer of "air" was added under the model. The effects of convection were not modeled on the sides or above the platform. It was assumed that the distance between the package lid and the top of the structure (> 1 millimeter) would result in negligible contributions to the convective heat loss when compared to the air layer below the platform. This assumption is based on the fact that the thermal resistance between the package lid and the plafrom is approximately 33 times larger than the thermal resistance between the bottom of the structure and the silicon below it. The heat loss from convection on the sides of the device was not modeled due to added complexity and is also expected to be much smaller than the heat loss due to the lower air layer. To perform the analysis three simulations were performed for each of the simulation conditions (Table 3). The effect of conduction was subtracted from the results in order to quantify the effect on oven gain due to convective and radiative heat loss. In addition, if we assume equal coverage of Al and AlN on the top of the device, the average emissivity of the top of the device should be around 0.5 This is based on

reported emissivities of Al and AlN in the range of 0.03 and 0.9 respectively [10-12]. The bottom and sides of the device consist of a thin film of SiO_2 with Silicon or metal underneath [13,14]. The emissivity of the entire OCMO structure is a complex combination of SiO_2, Al, AlN and other materials. Therefore to simplify the radiation model it was assumed that the average emissivity of all surfaces will fall in the range of 0.25 to 1. The results of these simulations are shown in Figure 16. The figure shows the oven gain of the structure accounting for both radiation and convection. It also shows the boundaries where convection and radiation limit the gain. Radiation clearly limits the oven gain once the pressure in the package is reduced. For an emissivity of one, convective and radiative heat loss are equal around 100 mTorr. Below that pressure radiation limits the oven gain to 100. With an emissivity of 0.5, the loss due to convection and radiation are equal at 50 mTorr and radiation ultimately limits the oven gain to 200. For our particular design we achieve package pressures on the order of 50 mTorr.

Table 3: Ansys Simulation Conditons

Measurement	Average Platform Emissivity	Package Pressure, Torr	Ambient temperature, °C
Conduction	0	0	0, 20, 40, 60 and 80
Radiation and Conduction	0.25, 0.5 and 1	0	0, 20, 40, 60 and 80
		0	0, 20, 40, 60 and 80
Convection and Conduction	0	0.01, 0.05, 0.1 and .5	0, 20, 40, 60 and 80
		0.01, 0.05, 0.1 and .5	0, 20, 40, 60 and 80
All	0.25, 0.5 and 1	0.01, 0.05, 0.1 and .5	0, 20, 40, 60 and 80
		0.01, 0.05, 0.1 and .5	0, 20, 40, 60 and 80

Based on the models results (Figure 16) the oven gain will not exceed much more than 100 for vacuum package pressure of 50 mTorr and an average emissivity of 0.5. Ultimately radiation limits the oven gain at low pressure (sub 1 mTorr) because of the current platforms' physical design. This design has a thermal resistance between the sense resistor and the oscillator. Therefore heat loss due to radiation causes a temperature dependent thermal gradient from the tip of the "finger" to the location of the sense resistance which is at a fixed temperature. In future designs it would be possible to create an improved platform design which would increase the limit on the oven gain by locating the temperature sensor closer to the resonator and oscillator electronics.

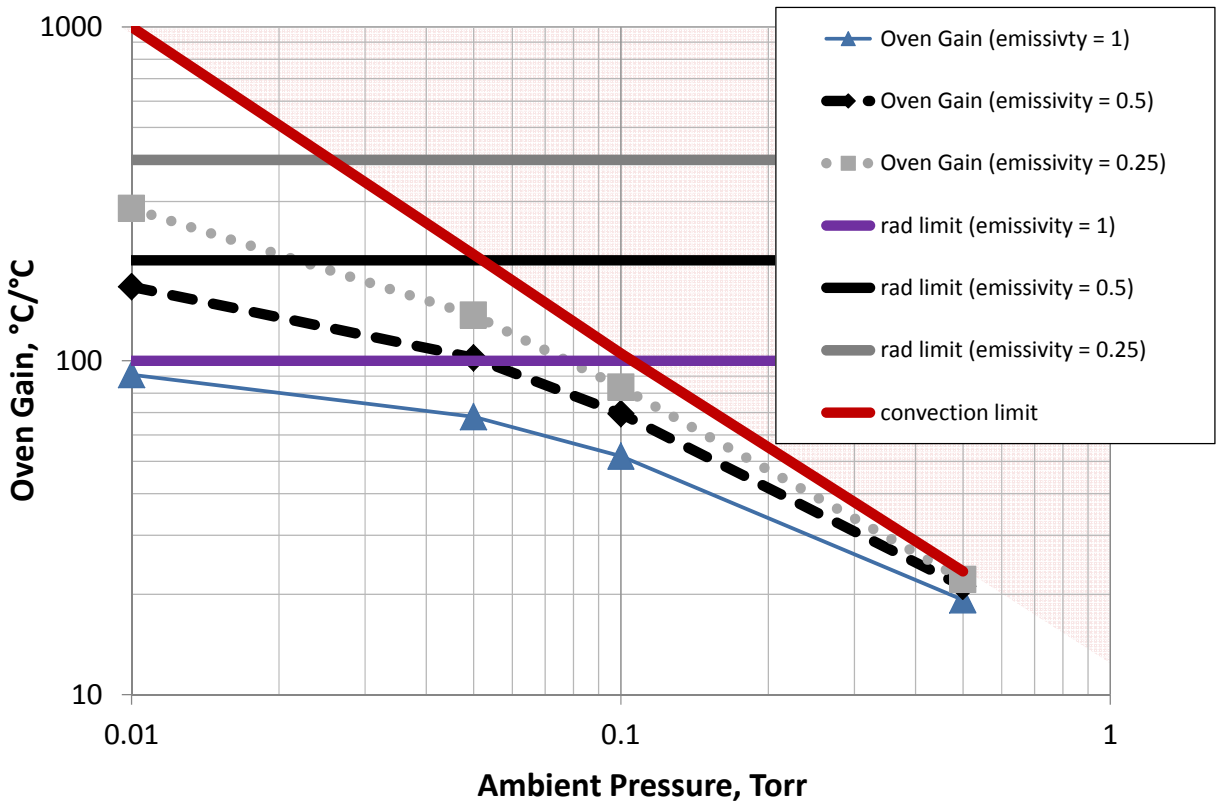

Figure 16: Simulated platform Oven Gain for the OCMO platform. The shaded area is the limit on oven gain set by convection. Oven gains in this area cannot be obtained with this design. The solid grey, black and purple lines are the limit on oven gain set by radiation for an average platform emissivity of 0.25, 0.5 and 1 respectively.

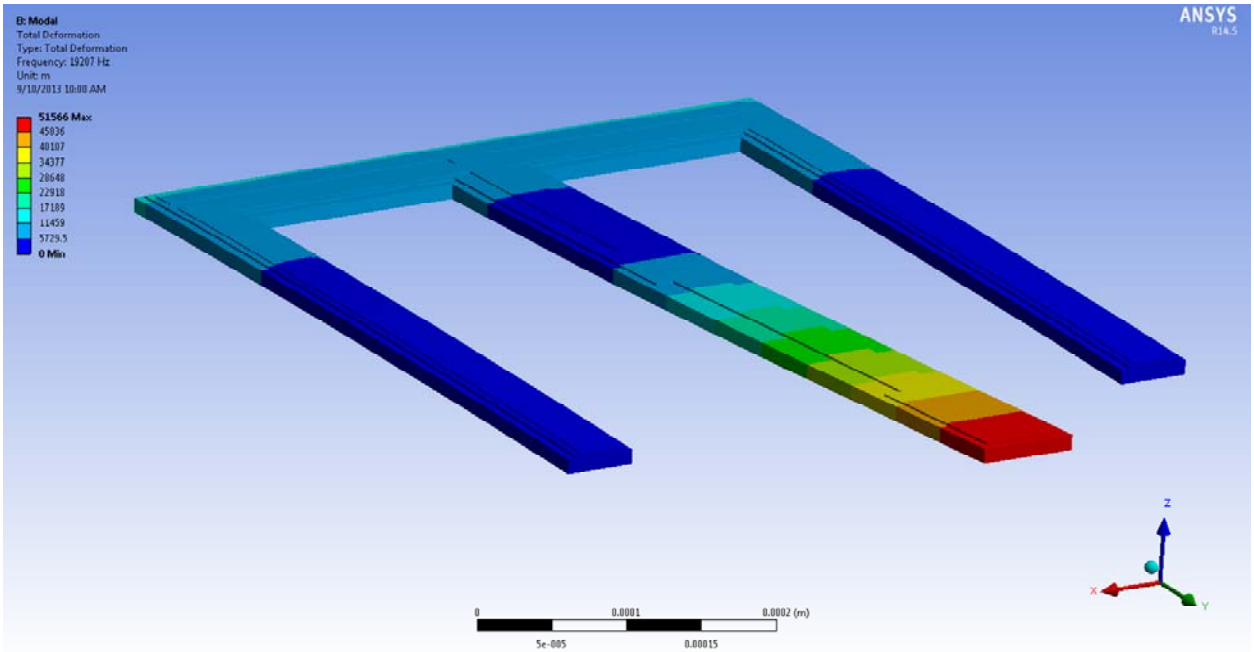

Figure 17. Result of ANSYS modal simulation showing the OCMO platforms first mode of oscillation is ~19 kHz.

Vibration stability or low sensitivity to environmental vibrations is also a goal for this LDRD. Typically the resonant frequency of the platform should be designed to be much greater than the vibration frequencies that will be experienced by the oscillator. Figure 17 is an ANSYS modal simulation result showing the fundamental mode of the platform. The fundamental mode was found to be 19 kHz which is much greater than the frequency of vibration seen by the oscillator in most applications. It should be noted that it is unclear that the oscillator would be sensitive to vibrations above or below 19 kHz unless it is tested.

2.4.2. OCMO Oscillator Design

The main goal the oscillator loop had to meet was the phase noise goal of -90 dBc/Hz at 1kHz offset referred to 1GHz. There were several goals and constraints in the oscillator design that determined the oscillator center frequency.

1. Resonator constraints:
    a. Size and frequency limited by the OCMO process. This is because the XeF_2 release process places a limit on the maximum width of the platform (50-70 μm). Typically, resonator frequency scales inversely with size. Phase noise is limited by the maximum power that can be applied to the resonator or resonator power handling. The maximum power or resonator power handling increases with increasing resonator frequency and size.
    b. Typically resonator Q is inversely proportional to its frequency. This relationship, however, is not strongly observed for AlN lamb wave resonators making oscillator operation at higher frequencies desirable because of the higher power handling.
    c. Past known good resonator designs with temperature compensation have been demonstrated in the 400 to 500 MHz range.

2. Oscillator Circuitry constraints:
    a. The oscillator circuitry has to be low power. This is because once placed on the OCMO platform it will actually cause the platform to heat up. Depending on the platform thermal resistance (10 to 20 degrees Celsius per mW) the temperature rise can be substantial (10-20 degrees Celsius).
    b. Oscillator power increases with frequency of operation.

3. Customers desired a frequency output in the range of 10-15 MHz.

Constraints on the resonator *TCF*, size, power handling and *Q* led to the choice of a resonator with a center frequency in the 400 to 500 MHz range. As a result, a Pierce oscillator topology was chosen for this design as it can operate at high frequency at very low power levels. In addition, a dynamic frequency divider [16] was added to provide an output signal at 10 to 15 MHz. The divider was designed to divide the oscillator frequency by 32 or 40. Finally, an automatic level control or ALC loop was added to the design to provide the option of internally controlling the peak-to-peak output voltage of the oscillator. It has been shown that the use of ALC can improve long term frequency stability. A block diagram of the oscillator is show in

Figure 18. The pin out of the OCMO IC is shown in the wire bonding diagram in Figure 19. In addition a description of the input/outputs including configuration logic is provided in Table 4.

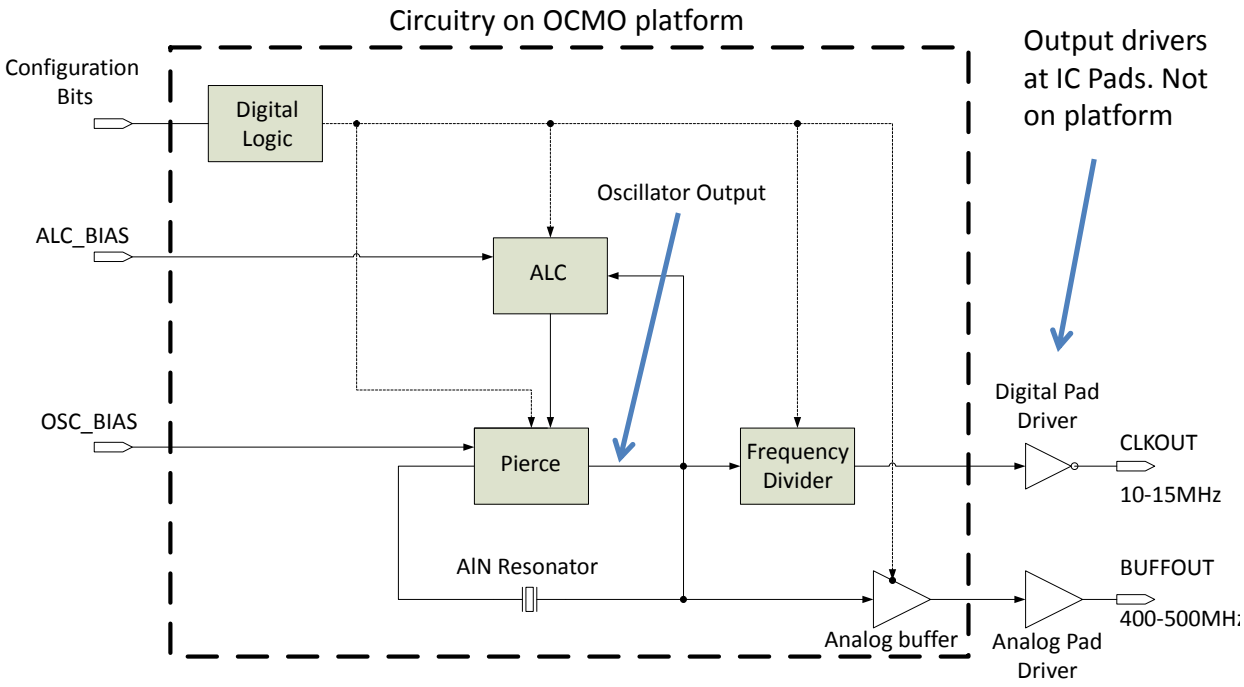

Figure 18. Oscillator circuitry on OCMO platform and digital/analog pad drivers.

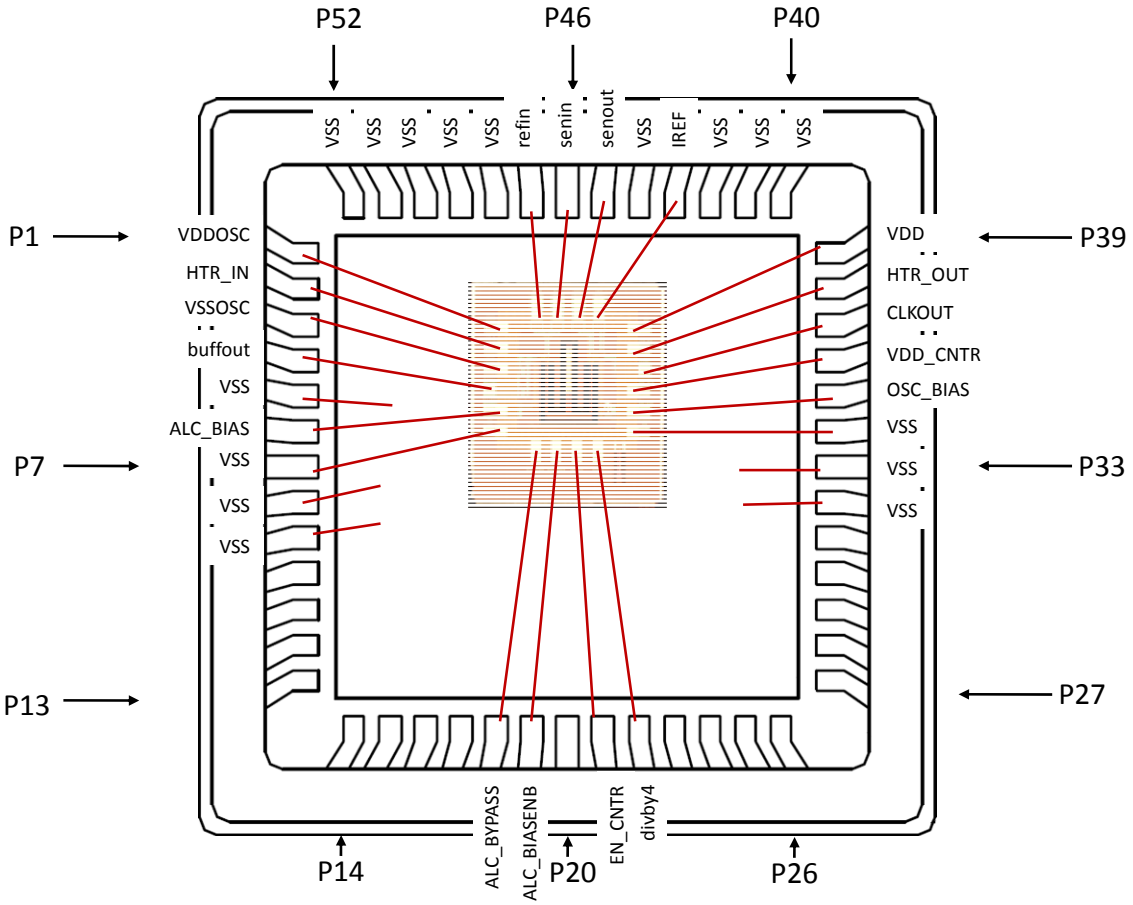

Figure 19. Wire bonding diagram of OCMO IC showing pin out.

Table 4: OCMO IC Inputs and Outputs (I/O).

Heater Control Loop I/O	
SENOUT	Connection to PCB based constant resistance temperature control loop, CRTCL.
SENIN	Connection to PCB based CRTCL.
REFIN	Connection to PCB based CRTCL.
IREF	Output of PTAT current source
HTR_IN	Connection to platform heater resistor. Connected to ground on PCB.
HTR_OUT	Connection to platform heater resistor. Driven by PCB CRTCL to heat the platform.
IC Power Supplies and Bias Currents	
VDDOSC	Oscillator Power, 3.3 V +/- .3V. This needs to be well regulated and supplied by a dedicated low TCV voltage reference.
VSSOSC	Oscillator ground. Can be shared with VSS
VDD	Power for digital output CLKOUT. Should be supplied by a separate 3.3 V voltage regulator.
VSS	Ground for digital output CLKOUT.
VDD_CNTR	Frequency Divider (counter) power supply. Set to 2V nominally. This needs to be well regulated and supplied by a dedicated low TCV voltage reference.
OSC_BIAS	Alternative bias current for oscillator. The oscillator current is equal to 4 times the current sunk from the OSC_BIAS pin. (Range = 0 to 200uA)
ALC_BIAS	Alternative bias current for ALC. Current should be sourced into this pad. Input range is 0 to 200uA

Oscillator Configuration Bits.	
ALC_BYPASS	Digital Input. If set high the ALC will be disabled. You must sink a current to ground on OSC_BIAS if set high.
ALC_BIASENB	Digital Input. If low the ALC level can be controlled externally with a current (sourced) into ALC_BIAS
Divby4	Digital input: If 0 divide oscillator frequency by 40. If 1 divide by 32 on CLKOUT.
EN_CNTR	Digital input. Enables CLKOUT. If high the BUFFOUT output is disabled.
Oscillator Outputs	
BUFFOUT	Analog output at oscillator frequency. Limited to 1-2pF load max.
CLKOUT	Digital output (divider output = 0 to 3.3V at oscillator frequency divided by 32 or 40.)

2.4.3. PCB and Temperature Control Loop Implementation

Two printed circuit boards, PCBs, were designed to enable testing of the OCMO. The main PCB was designed with a socket enabling a daughter board with an OCMO oscillator to be plugged into the main board. This enabled testing of multiple OCMO oscillators with the same main PCB (Figure 20). Each daughter board has commercial off-the-shelf, COTS, based buffers for both output of the OCMO: BUFFOUT and CLKOUT. These buffers are capable of driving the 50 ohm input impedance which is standard for most test equipment used to characterize the oscillator. The main PCB contains the constant resistance temperature control loop (described in section 2.2.2) The loop forces the sense resistance R_s to be equal to a reference resistor, R_{ref}. The control loop is shown in Figure 21. The control loop consists of two AD8638 opamps.

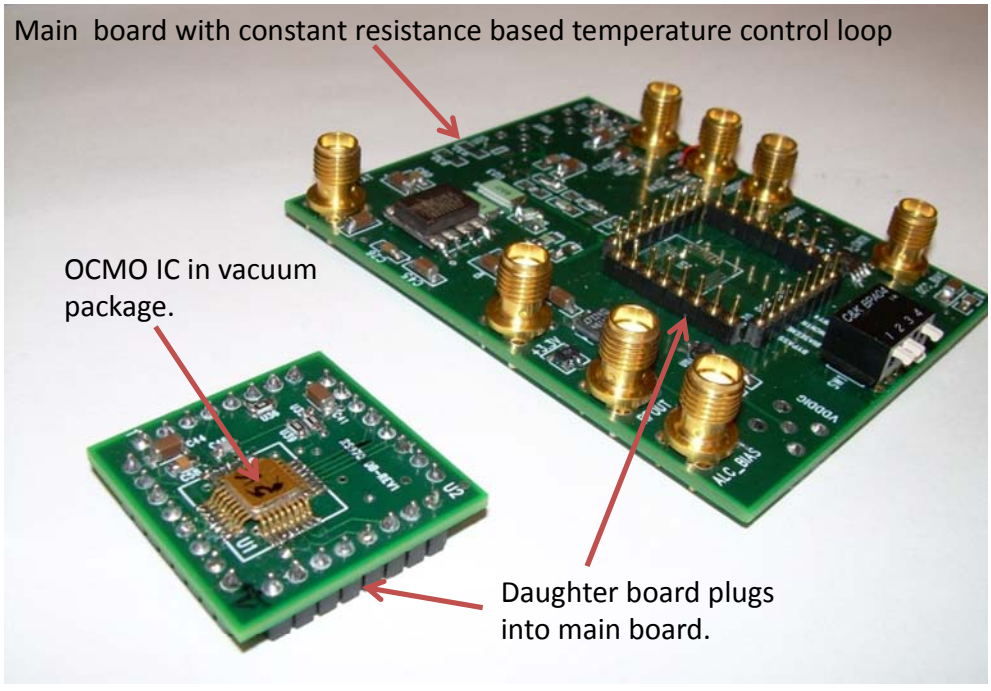

Figure 20: Photograph of PCBs developed to test the OCMO IC.

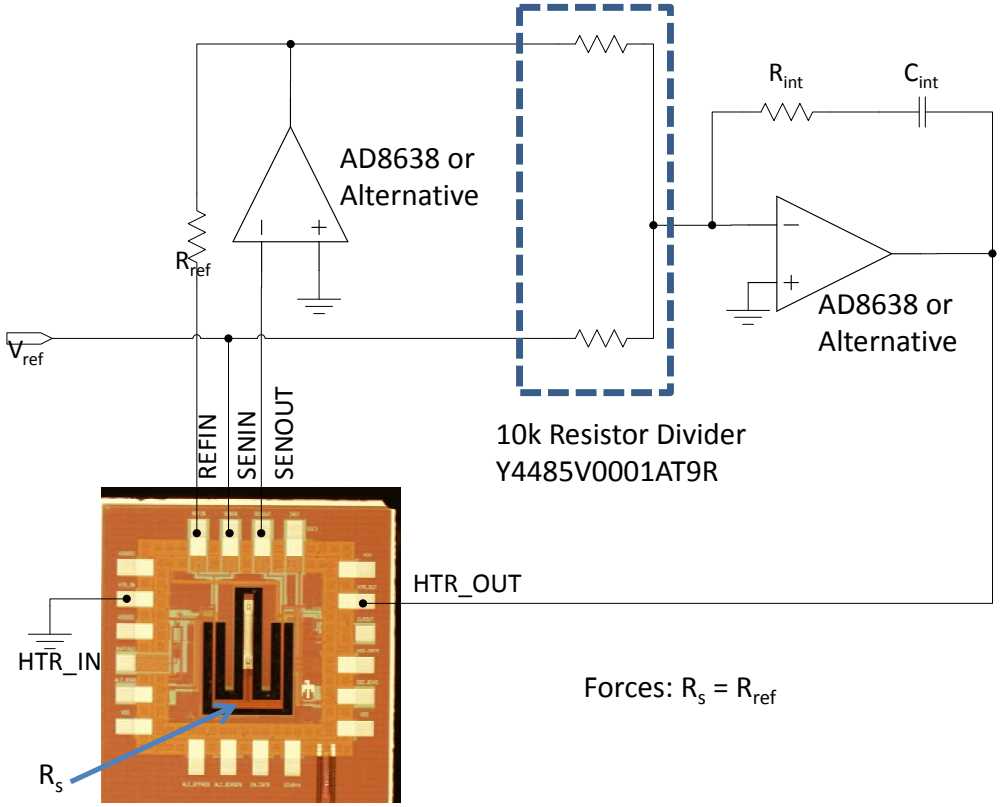

Figure 21. PCB based constant resistance temperature control loop, CRTCL.

3. OCMO MEASUREMENT RESULTS

3.1. Typical Resonator Characteristics.

The resonator used in the OCMO design was a width extensional resonator with a center frequency of around 480 MHz. The typical resonator measured had an insertion loss of –9 dB and a Q = 1900. The oxide layer under the resonator was designed to minimize its temperature coefficient of frequency. The temperature coefficient of frequency cannot be measured directly on the OCMO IC. As a result, it is measured by measuring the OCMO oscillator frequency versus temperature with the temperature control loop disabled. This will be shown in the next section.

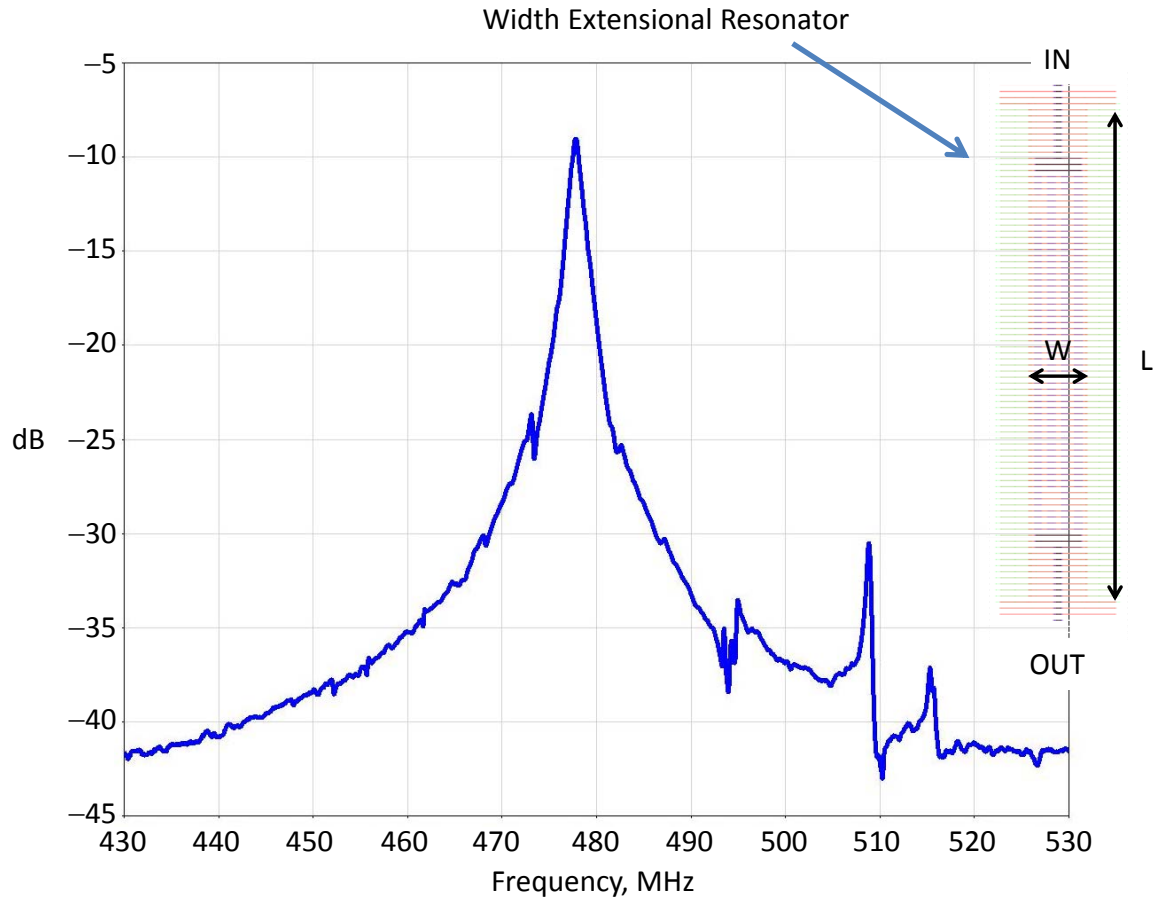

Figure 22. S_{21} measurement of a typical width extensional resonator and a picture of its layout. Resonator size: length, L = 287μm and width, W = 32μm

3.2. Temperature Sensitivity of OCMO

To characterize the OCMO temperature sensitivity, the output of the oscillator was first measured with the constant resistance temperature control loop disabled. The results of this measurement are shown in Figure 23. It shows that the oscillator exhibits frequency versus temperature which is parabolic. The vertex of the parabola defines the turnover frequency and temperature. The turnover temperature for this particular oscillator is ~83 degrees Celsius. At the turnover temperature the temperature coefficient of frequency for the oscillator is zero. This

nonlinear frequency versus temperature characteristic is typical of temperature compensated resonators [8]. Since the oscillator power heats the OCMO platform above the ambient temperature, the resonator and oscillator electronics are operating at a higher temperature than the measured oscillator turnover temperature. Based on measurement, the actual resonator turnover temperature is ~ 97.8 degrees Celsius. Therefore, if the thermal control loop is set to keep the resonator and electronics at this temperature the TCF of the oscillator can be minimized. To set the temperature of the oscillator, the sense resistor must be characterized over temperature (Figure 24).

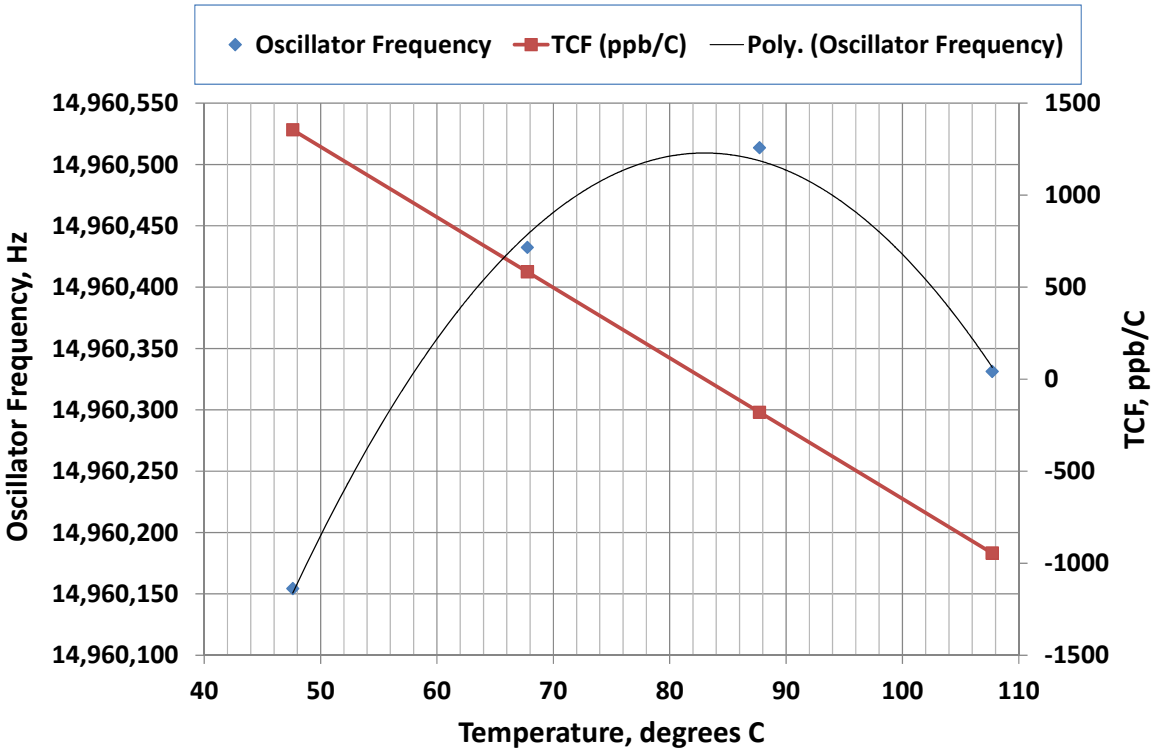

Figure 23. OCMO frequency versus temperature with the control loop disabled. The turnover temperature is ~ 83 degrees Celsius.

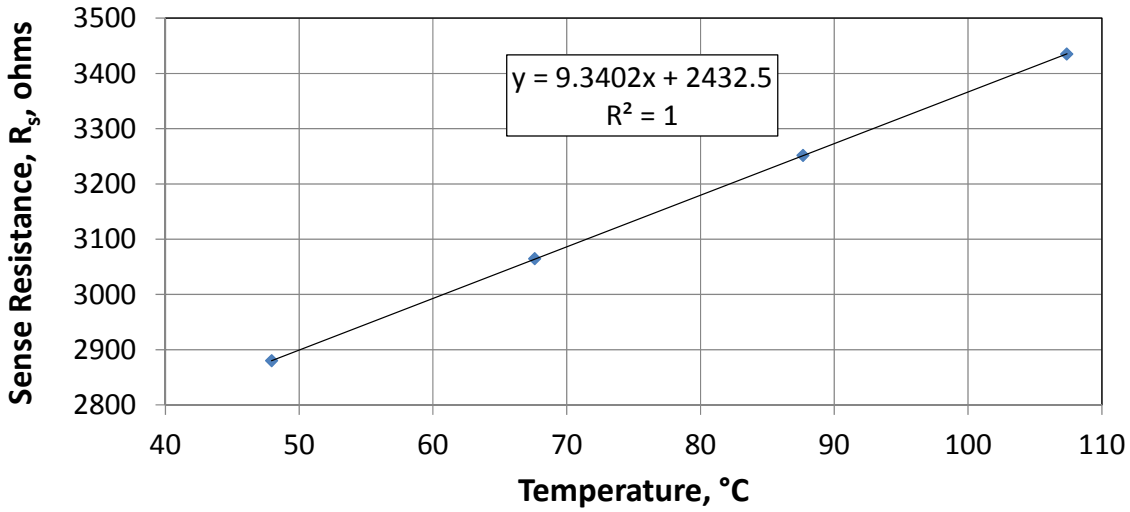

Figure 24. Sense resistance, R_s, versus temperature.

The value of R_{ref} was calculated to be 3382 ohms and was placed in the main PCB control loop. The temperature control loop was turned on and the oscillator TCF was re-measured. The temperature was cycled from 30°C to –40 °C. Then it was ramped from –40 to 85°C. Finally, the oven temperature was ramped back down to 30°C. The temperature profile applied to the resonator is shown in Figure 25 (right axis). T_{oven} (red) is the oven set point and T_{lid} (blue) is the temperature of the OCMO package lid. Note that the oscillator's frequency drift was removed from the measurement in Figure 25 to determine the temperature sensitivity of the OCMO. This was done by taking the values of frequency at *Toven* = 30 °C versus time and fitting a 3rd order polynomial to the drift (Figure 25).

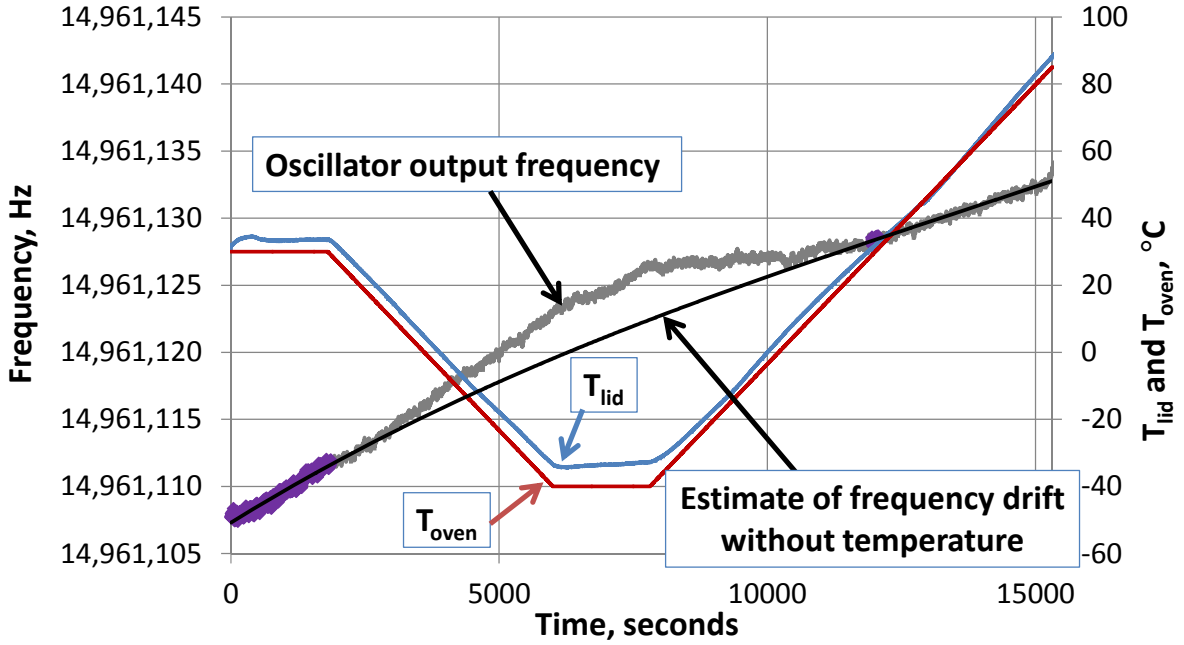

Figure 25: Oscillator frequency measurement made in a Rasko oven. The frequency Drift is estimated from this measurement by using a least squares fit to frequency data taken at 30 °C during the measurement (shown in purple).

The solid black line (Figure 25) is the estimate of the oscillators frequency drift in the absence of changes in oven temperature. Hence this estimate predicts the time variation of the oscillator frequency for a fixed temperature of 30°C. The estimate of drift was then subtracted from the measurement to obtain the results shown in Figure 26. An insulating material was placed on top of the PCB during the test to protect it from liquid CO_2 and transient changes in oven temperature due to the turbulent atmosphere in the oven. This allowed the power dissipated by the PCB to heat the PCB and package above the oven temperature. This accounts for the difference between T_{lid} and T_{oven} (Figure 25). In addition, it is important to note that this measurement was taken with all of the oscillator power supply regulators inside the oven. Therefore, it combines frequency variation due to the power supply regulators' voltages changing over temperature with the intrinsic oscillator temperature variation. Future experiments will remove the regulators from the oven to measure the intrinsic oscillator temperature coefficient. However, this experiment shows how the device would operate in a "real world" situation where all components are subject to temperature variation. From this measurement, the overall fractional frequency variation, $\Delta f/f_o$, was determined to be ~ 250 ppb over the

temperature range of –40 to 85°C and ~90 ppb from 0 to 85°C. It can be seen from this plot that the majority of variation (~160 ppb) occurs between the temperatures of –40 and 0°C.

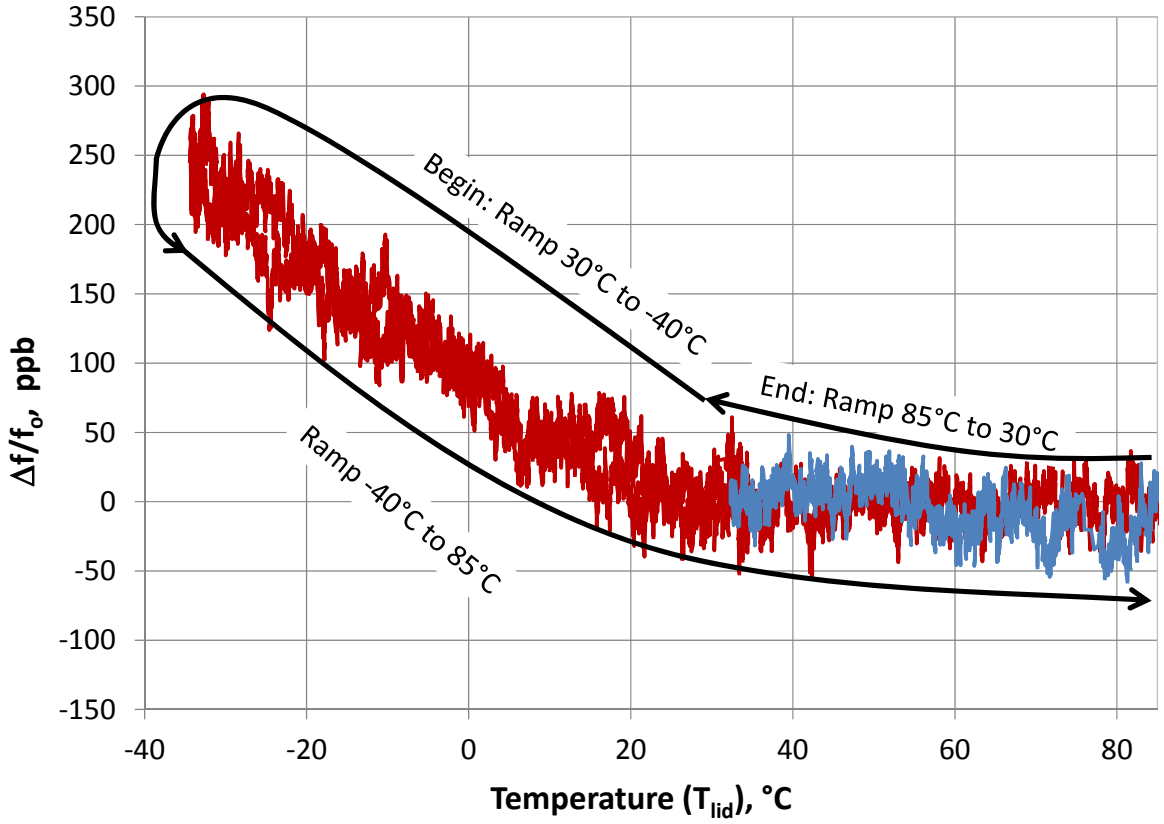

Figure 26: Measurement of OCMO temperature coefficient, TCF.

It is important to note that the control loop oven gain was on the order of 100 for this oscillator. This is because of either poor vacuum in the package or radiative heat loss. However, this oscillator still meets the LDRD goal because we are operating at the turnover point. Thus, this design is robust even with oven gain limited by convective and/or radiative heat loss. The thermal time constant of the OCMO platform was measured by sweeping the frequency, f_H, of a fixed amplitude sinusoidal voltage applied to the heater resistor. Since the platform temperature is a function of the power ($P_H=V_H^2/R_H$) applied to the heater resistor, the resulting platform temperature varies at a frequency equal to twice the applied frequency, f_H. Therefore, by observing the change in the sense resistance, R_s, at $2\times f_H$, the thermal transfer function of the platform was measured. The most important parameter obtained by this measurement was the platforms thermal time constant, $R_{th}\times C_{HC}$. The thermal time constant is equal to the product of the thermal resistance and heat capacity of the platform. Where R_{th} is the platform's thermal resistance and C_{HC} is its heat capacity. The change in platform temperature was measured with the sense resistor, R_s, through use of an inverting amplifier (Figure 27). The amplifier output spectrum at $2\times f_H$ was observed with a spectrum analyzer and the amplitude of its output was recorded. Using this method, the thermal time constant of the OCMO platform was found to be ~13.6 milliseconds (Figure 28). This allows the feedback loop for the OCMO to react much more quickly to thermal transients than large quartz crystal based TCXOs and OCXOs.

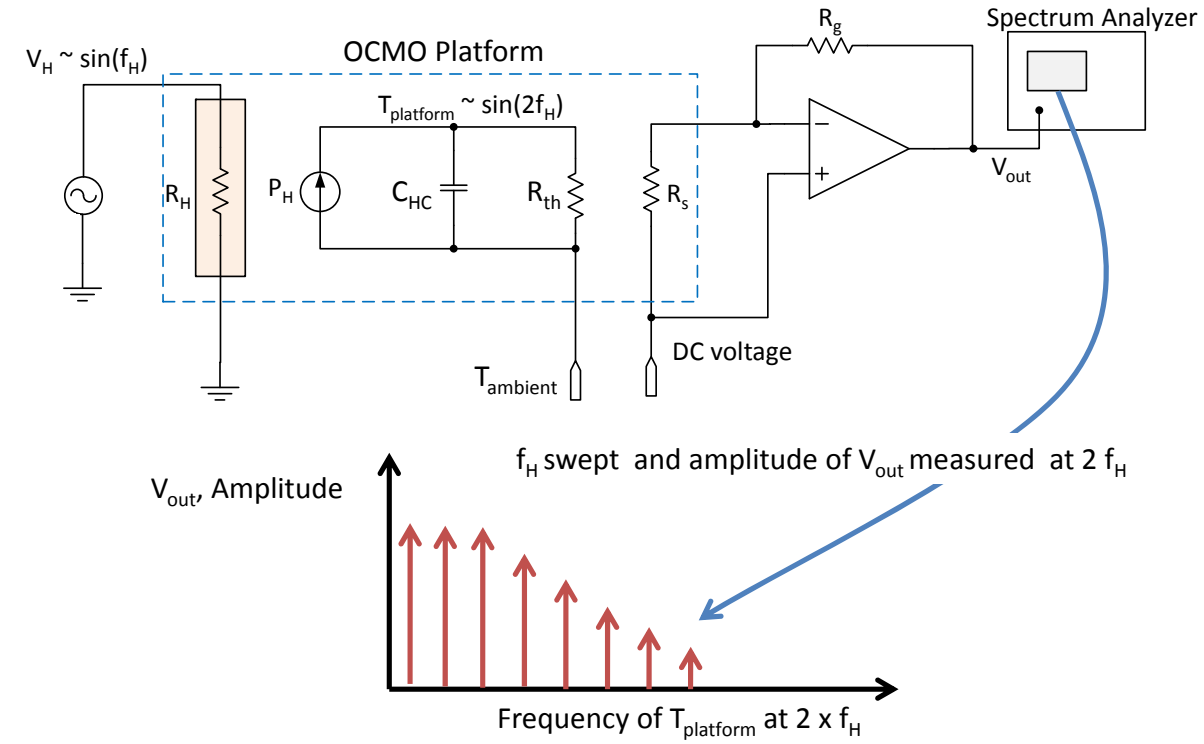

Figure 27: Method used for measurement of the platforms thermal time constant.

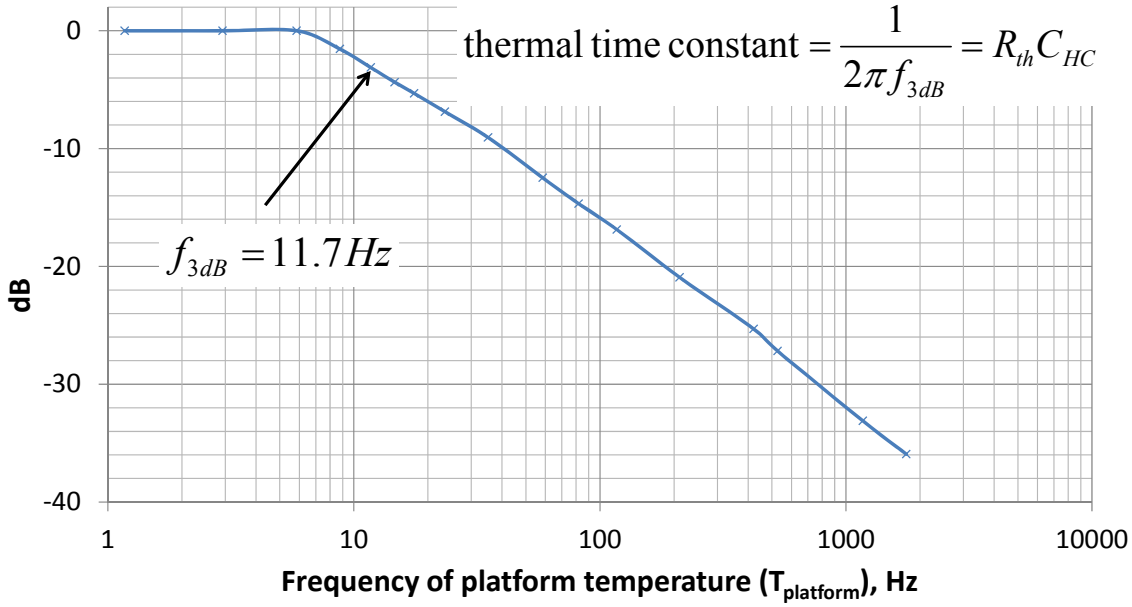

Figure 28: Measurement of OCMO thermal response versus frequency of the heater power applied to the structure. The 3dB frequency was found to be 11.7 Hz.

3.3. OCMO Phase Noise

The phase noise at the CLKOUT output of the oscillator (divider set to divide by 32) was measured to be -123.8 dBc/Hz at 1kHz offset (Figure 29). The center frequency was ~15 MHz.

Therefore the phase noise referred to 1 GHz is -87 dBc/Hz. Further improvements in phase noise will require increasing the quality factor of the AlN resonator.

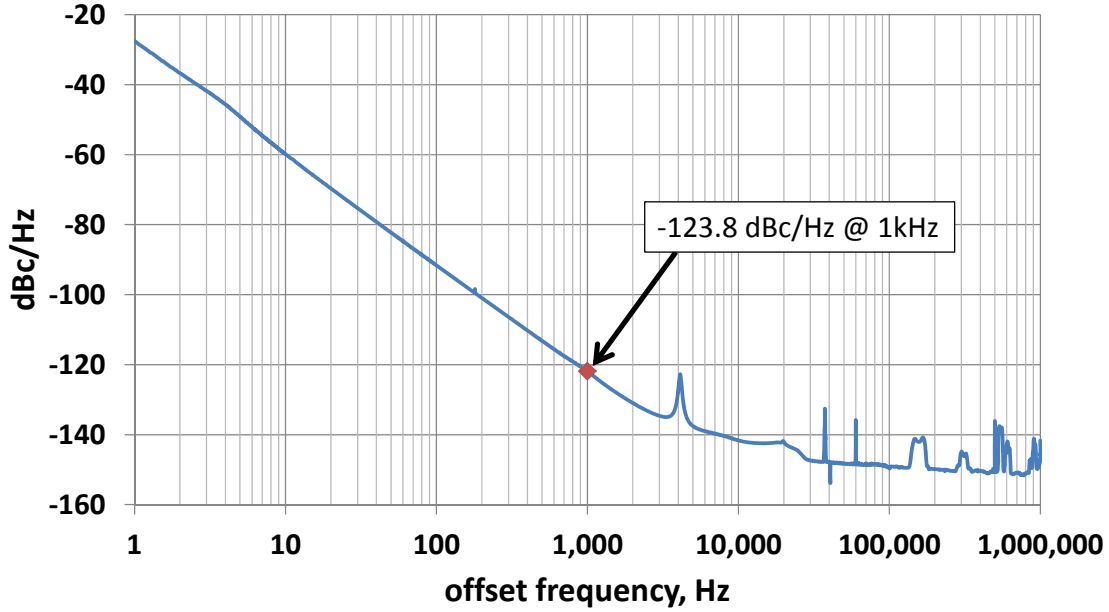

Figure 29: Phase noise of the OCMO oscillator measured with a Symmetricom 5125A phase noise analyzer, PNA. A Stanford Research Systems FS725 rubidium frequency standard was used for the 5125A's frequency reference.

3.5. OCMO Power

Table 5: OCMO Power Breakdown

Component	Supply Voltage (V)	Supply Current (mA)	Power (mW)
Pierce Oscillator	3.3	0.177	0.58
Frequency Divider	2.05	0.324	0.66
CMOS Pad Driver (10 pF load at 15 MHz)	3.3	1.212	4.00
OCMO platform heater power at room temperature	1.08	5.400	5.83
OCMO subtotal			11.08
Un-optimized COTS CRTCL	10	2.000	20.00
Total (un-optimized CRTCL power)			25.83
Optimized COTS CRTCL	3.3	0.200	0.66
Total (optimized CRTCL power)			11.74

A breakdown of the power used by the OCMO oscillator developed in this work is shown in Table 5. The breakdown shows the total power of the OCMO at room temperature (7.4 mW). The OCMO subtotal is the power used by the pierce oscillator, frequency divider, pad drive and the platform heater. The heater power is the amount needed to heat the OCMO platform to 85 C at ambient temperature (5.83 mW). The total power adds the COTS based constant resistance control loop power to the OCMO power. As can be seen, the PCB based control loop power

dominates the total power used by the oscillator. This power could easily be reduced to ~0.7 mW by reducing the COTs control loops' power supply voltage to 3.3V and by using operational amplifiers with nominal supply currents of 0.1 mA. In the future we expect to integrate the control loop on the OCMO IC. This could conceivably reduce the power used by the loop electronics even further than the power estimate of 0.7 mW in Table 5. Basically the power used to heat the platform will dominate.

3.6. Frequency Stability

An important characteristic for frequency references is the rate at which their frequency changes over time. The Allan deviation or ADEV is used to evaluate the stability of an oscillator over a given measurement time, tau [17,18]. The ADEV of an oscillator provides the normalized standard deviation or root mean square change in the references fractional change in frequency over a given measurement time tau. To quote [18]: "An Allan deviation of 1.3×10^{-9} at observation time 1 second (i.e. $\tau = 1$ second) should be interpreted as there being an instability in frequency between two observations a second apart with a relative root mean square (RMS) value of 1.3×10^{-9}. For a 10-MHz clock, this would be equivalent to 13 mHz RMS movement." Figure 30 shows the measured ADEV for the OCMO. This measurement shows the standard deviation of the OCMO oscillator frequency to be ~5 ppb for tau = 1 second. At approximately 1000 s the ADEV starts to increase due to long term frequency drift. In the case of the OCMO this drift is aging which is believed to be caused by the metal in the AlN resonator going through nonlinear deformations (creep, work hardening). It has been observed that this aging/drift slows the longer the oscillator is in operation. Thus, a burn-in period is required to reduce the drift to an acceptable level. Further investigation is required to determine the root cause of the frequency drift and identify ways of reducing it further.

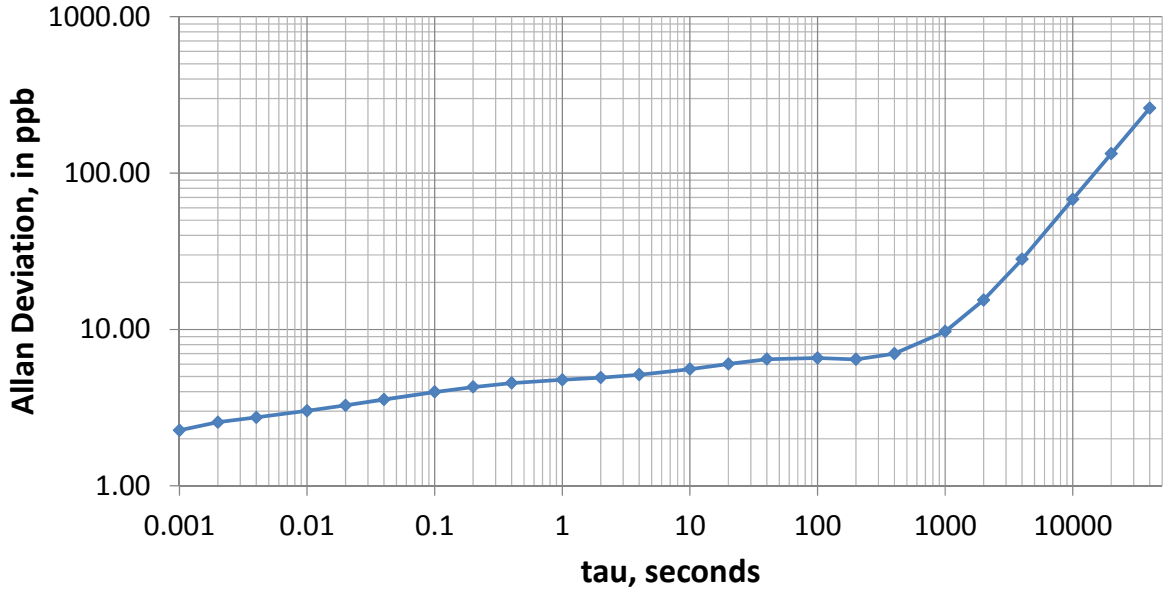

Figure 30: Allan deviation measurement for the OCMO oscillator. Measurement time ~ 11 hours.

4. CONCLUSIONS

In this LDRD we have shown it is possible to make a MEMs based oscillator that has 100x better vibration stability, uses 50x less power, is >100x smaller while having similar temperature stability when compared to today's state of the art crystal oscillators (Table 6). We believe this is an exceptional achievement considering the funding level and development time of this LDRD.

Table 6: LDRD Accomplishments

Vendor Product	Technology	Frequency (MHz)	Phase Noise 1kHz offset (dBc/Hz) ref. 1 GHz	Vibration Sensitivity (ppb/G)	Power (mW)	Temp. Coeff. (ppb/°C)	Volume (mm^3)
Rakon RFPO40	Ovenized Quartz (OCXO)	10.94	-105	2	400	±0.5 to 2	313
This LDRD	Ovenized Piezo MEMS (OCMO)	15	-87	1.2	11.7	± 0.8	0.06-1

4.1. Future Directions

While much has been achieved under this development effort, particularly in the area of thermal stability, more development work is required in order to field these oscillators' in future applications.

A bulleted list of recommend further research is below, the priority of which will be application dependent.

- Improve oven gain to further improve the oscillator thermal stability. This can be done by improving the vacuum level or by placing the resistive temperature sensor in more intimate thermal contact (i.e. closer to) with the resonator.
- Wafer Level Packaging for the oscillator. This would enable ultra-small/thin oscillators.
- Improve control of temperature at which TCF turnover point occurs. Prior work on engineering the passive resonator TCF has focused on filtering applications and placed little importance on the turnover temperature. Study of how to engineer the turnover temperature will be critical to achieving the lowest possible power consumption for a given application (i.e. maximum operating temperature).
- Discover the source of the frequency drift requiring long burn in times and mitigate it. This is perhaps the most important research required prior to application of this technology.
- Increase the resonator Q to improve phase noise and short term Allan deviation.
- Integrate the oven control loop circuitry on the integrated circuit die to minimize size and power consumption.
- Implement a frequency trimming approach for tuning the initial accuracy of the oscillator post-fabrication.

5. REFERENCES

1. R. Brendel, G. Marianneau, F. Djian, E. Robert, "*Improved OCXO's Oven Using Active Thermal Insulation*," IEEE Transactions on Ultrasonics, Ferroelectrics, & Frequency Control, Vol. 41, No. 2., pp. 269 – 274, March 1994.
2. Mike F. Wacker, David A. Villella, "*Improvements in OCXO performance by the use of an on-board microprocessor*," 2008 IEEE International Frequency Control Symposium, pp.159,164, May 2008.
3. R. H. Olsson III, K. E. Wojciechowski, M. R. Tuck, J. E. Stevens and C. D. Nordquist, "*Multi-Frequency Aluminum Nitride Micro-Filters for Advanced RF Communications*, " Govt. Microcircuit App. and Critical Tech. Conf., pp. 257-260, March 2010.
4. K. E. Wojciechowski, R. H. Olsson, M. R. Tuck, E. Roherty-Osmun, T. A. Hill, "*Single-chip precision oscillators based on multi-frequency, high-Q aluminum nitride MEMS resonators*," 2009 Solid-State Sensors, Actuators and Microsystems Conference, pp. 2126-2130, 2009.
5. E.A Vittoz, M. G. R. Degrauwe, S.Bitz, "*High-performance crystal oscillator circuits: theory and application*," IEEE Journal of Solid-State Circuits, vol.23, no.3, pp.774-783, June 1988.
6. R.K. Karlquist,"*A new type of balanced-bridge controlled oscillator*," IEEE Transactions on Ultrasonics, Ferroelectrics and Frequency Control, vol.47, no.2, pp.390,403, March 2000.
7. B. Kim, J. Nguyen, K.E. Wojciechowski, R. H. Olsson, "*Oven-Based Thermally Tunable Aluminum Nitride Microresonators*," Journal of Microelectromechanical Systems, vol.22, no.2, pp.265,275, April 2013.
8. R. Melamud, B. Kim, M.A. Hopcroft, S. Chandorkar, M. Agarwal, C.M. Jha, T. W. Kenny, "*Composite flexural-mode resonator with controllable turnover temperature*," IEEE 20th International Conference on Micro Electro Mechanical Systems, pp.199-202, Jan. 2007.
9. B Kim, R. H. Olsson, K. Smart, K. E. Wojciechowski, "*MEMS resonators with extremely low vibration and shock sensitivity*," 2011 IEEE Sensors, pp.606-609, Oct. 2011.
10. Olivier Riou, Pierre-Olivier Logerais, Jean-Félix Durastanti, "*Quantitative study of the temperature dependence of normal LWIR apparent emissivity*", Infrared Physics & Technology, Volume 60, Pages 244-250, September 2013.
11. R, Abbot, S. Waldman, "Thermal Coatings for In-vacuum Radiation Cooling", Laser Interferometer Gravitational-Wave Observatory Report, LIGO-T070054-00-C, March 2007.
12. C. H. Jenkins, "Recent advances in gossamer spacecraft," Reston, VA: American Institute of Aeronautics and Astronautics, ISBN: 1563477777, 2006.
13. S. Abedrabbo, N. M. Ravindra, W. Chen, V. Rajasekhar, T. Golota, O. H. Gokce, A. T. Fiory, B. Nguyenphu, A. Nanda, T. Speranza, W. Maszara, G. Williamson, "Temperature Dependent Emissivity of Multilayers on Silicon," MRS Proceedings, 1997.
14. N. Ravindra, K. Ravindra, S. Mahendra, B. Scopori, A. Fiory, "*Modeling and simulation of emissivity of silicon-related materials and structures*," Journal of Electronic Materials, Vol. 32, Issue 10, pp 1052-1058, 2003.

15. B Kim, R. H. Olsson, K. E. Wojciechowski, "Ovenized and thermally tunable aluminum nitride microresonators," *Ultrasonics Symposium (IUS), 2010 IEEE* , vol., no., pp.974,978, 11-14 Oct. 2010.
16. Ching-Yuan Yang; Guang-Kaai Dehng; June-Ming Hsu; Shen-Iuan Liu, "*New dynamic flip-flops for high-speed dual-modulus prescaler*," IEEE Journal of Solid-State Circuits, vol.33, no.10, pp.1568-1571, Oct 1998
17. D. W. Allan, "*Statistics of atomic frequency standards*," Proceedings of the IEEE , vol.54, no.2, pp.221-230, February 1966.
18. (on-line) http://en.wikipedia.org/wiki/Allan_deviation#Allan_deviation

DISTRIBUTION

1	MS0101	David R. Sandison	00110
1	MS0509	Dahlon Chu	05330
1	MS0519	Richard C. Ormesher	05332
1	MS0529	Jayson A. Payne	05332
1	MS0532	Bert L. Tise	05348
1	MS0621	Dallas Wiener	05632
1	MS0621	Vincent M. Hietala	05638
1	MS0628	David A. Wiegandt	05333
1	MS1069	Roy H. Olsson III	01719
1	MS1069	Michael S. Baker	01719
1	MS1071	Rita A. Gonzales	01750
1	MS1072	Fredrick W. Sexton	01752
1	MS1072	Kenneth E. Wojciechowski	01752
1	MS1202	Reid S. Bennett	05955
1	MS1209	Michael T. Valley	05955
1	MS0359	D. Chavez, LDRD Office	01911
1	MS0899	Technical Library	09536 (electronic copy)


Sandia National Laboratories